Structures 38 (2022) 599–617

Contents lists available at ScienceDirect

Structures

journal homepage: www.elsevier.com/locate/structures

Analysis of the soil structure-interaction effects on the seismic vulnerability of mid-rise RC buildings in Lisbon

M.V. Requena-Garcia-Cruz [a,*], R. Bento [b], P. Durand-Neyra [a,c], A. Morales-Esteban [a,c]

[a] Department of Building Structures and Geotechnical Engineering. University of Seville, Av. Reina Mercedes, 2, 41012 Seville, Spain
[b] CERIS, Instituto Superior Técnico, Universidade de Lisboa, Av. Rovisco Pais, 1049-001 Lisbon, Portugal
[c] Instituto Universitario de Arquitectura y Ciencias de la Construcción. University of Seville, Av. Reina Mercedes, 2, 41012, Seville, Spain

ARTICLE INFO

Keywords:
Seismic vulnerability
Reinforced concrete buildings
Soil-structure interaction (SSI)
3D finite elements
Beam on Nonlinear Winkler method (BNWM)
Direct method

ABSTRACT

Soil-structure interaction (SSI) effects are usually omitted in the seismic vulnerability analyses of buildings. However, it has been proved that they might notably affect their seismic performance. In fact, European seismic codes establish that they should be included in the analyses of certain structures: with considerable second order (p-Δ) effects or mid/high-rise buildings. These characteristics are shared by reinforced concrete (RC) buildings in Portugal, which represent a considerable amount of its building stock. Moreover, a significant percentage (50%) have been constructed prior to restrictive seismic codes, i.e., without adequate seismic design. To obtain reliable results when including the SSI effects, the state-of-the-art reveals that a proper modelling of soil and foundations should be carried out. Nevertheless, most of the related studies are based on ideal structural and soil configurations. In addition, it has been found that there is a lack of studies and guidance, even in codes, on the quantification of the SSI effects. Therefore, this paper focuses on quantifying the SSI effects in RC buildings seismic vulnerability analyses by means of two approaches: the Beam on Nonlinear Winker method (BNWM) and the direct modelling of soil. The aim is to propose a method to practically include the SSI effects and to thoroughly characterise the soil behaviour. The method has been applied to a case study RC mid-rise building of Lisbon. A clay-type soil commonly found in Lisbon has been characterised, carrying the analyses out under undrained conditions. 3D finite elements procedures have been proposed to reproduce the complex soil nonlinear constitutive law to represent the behaviour of the entire system (soil + foundation + structure) as realistically as possible. The results have been compared in terms of the seismic safety verification and the fragility assessment. The results have shown that the modal behaviour and the deformed shape of the building are the same with and without the SSI. Nonetheless, it has been demonstrated that increasing the soil flexibility leads to higher periods and higher seismic damage. For this case study, the maximum capacity of the models can be reduced by up to 15% if the SSI effects are considered.

1. Introduction

The soil under the buildings is usually ignored in seismic vulnerability analyses. Despite its importance in the building construction, its consideration in seismic analyses remains unclear. In fact, the soil-structure interaction (SSI) was assumed to be beneficial in past research [1] due to the reduction of internal forces and drifts owing to the increased flexibility of the soil. Hence, the seismic analyses were carried out considering fixed-base buildings to obtain conservative results. However, studies on the influence of the SSI in the capacity assessment of buildings proved that it does not positively affect all types of buildings in all types of soil [2]. In fact, it can be intuitively assessed that structural and ground displacements are not independent of each other [3]. In this sense, part-1 of Eurocode-8 (EC8-1) [4] suggests that the soil affectivety needs to be considered when structures present significant second order (p-Δ) effects, are slender or are mid/high-rise buildings. Moreover, it was proved that the SSI might affect aspects related to the seismic performance of buildings such as the ductility, the strength [5] or the energy dissipation [6]. Therefore, for certain cases, if the SSI is omitted, the results can lead to overestimating the capacity of the structures, resulting in unreliable results.

Most of the reinforced concrete (RC) buildings located in Lisbon are mid-rise buildings constructed prior to the restrictive Portuguese seismic code [7]. Hence, most of them were only designed considering the

* Corresponding author.

https://doi.org/10.1016/j.istruc.2022.02.024
Received 25 November 2021; Received in revised form 10 January 2022; Accepted 9 February 2022
Available online 16 February 2022

gravitational loads and omitting more complex aspects, such as the p-Δ effects and lack an adequate seismic criterion. They represent 71% of the total of RC buildings (52 496) in Portugal [8]. Owing to these characteristics, much effort was thoroughly made in their seismic assessment [9–11]. However, despite the fact that they might be affected by the SSI effects, these have not been borne in mind.

The literature review reveals the lack of RC building seismic vulnerability analyses including the SSI, despite the fact that they can affect their response [1]. It has been found that there is a tendency in using automatic methods based on Artificial Intelligence to model the soil and the foundations. However, most of them propose limited and simple modelling approaches. These are even based on ideal structural configurations and soil parameters: bare-frame fictional configurations and without characterising the soil. However, in order to obtain reliable results, a proper modelling of the soil and foundations is needed as extensively stated by the available literature. Therefore, they might not be able to properly assess the real affectivity of the SSI. Moreover, they do not take into account aspects that affect their seismic vulnerability: the dimensions and the joints of structural elements, the geometry, the presence of smooth rebars or the irregularities in plan and in height due to the infills' influence.

The SSI effects are taken into account by modifying the flexibility at the base of the buildings. There are several approaches to model this soil flexibility [3] based on simplified or exhaustive models. Some well-known simplified models for capturing the nonlinear behaviour of the soil-foundation system are the Beam on Nonlinear Winkler method (BNWM), the lumped spring models [12] or the constitutive models. One of the constitutive models, which is referred to as a macro-element, has been widely discussed in several works [13–15]. This approach can capture the nonlinear behaviour of the soil with lumped nodes. It is a modelling option that provides an efficient model with relatively few required parameters compared to other models such as 3D.

Although the macro-element concept has indeed been thoroughly used, it has not yet been implemented in new earthquake engineering software. To do so, correlation studies with available experimental tests are needed to demonstrate the model performance as proved by Ramirez et al. [16]. In this work, some soil hypoplastic materials have been numerically tested to be implemented in open-source software such as OpenSees. Moreover, specific algorithms to model this approach should also be developed. In Hyeon Chai and Kwon [17], they were briefly introduced. Nevertheless, this is not the goal of the present work. Therefore, in this case, two of the most common approaches have been used to model the SSI: a simplified and an exhaustive approach, the BNWM and the direct, respectively.

The BNWM has been accepted in engineering practice due to its relative simplicity and ease of calibration [18]. It is based on the modelling foundation's elements as well as simulating the nonlinear behaviour of the soil by means of a set of inelastic springs. These materials were firstly proposed for the analysis of piles [19]. In fact, there are several works on the determination of piles behaviour (isolated) considering these elements [20]. Nevertheless, to the best of the authors' knowledge, there are very few studies that model the entire system's behaviour (soil + pile + structure) [21].

The BNWM materials have been also developed to be used in shallow foundations analyses [22]. In Rajeev and Tesfamariam [23], fragility curves for ideal RC bare-frame structures were obtained considering the SSI. The fragility curves derived from the fixed-model differ from the SSI models depending on the nature of the structure. They concluded that in order to obtain reliable results, these analyses should be carried out considering the characteristics and the configuration of the existing buildings. A single shallow foundation was experimentally and numerically assessed bearing in mind soil uncertainties in Raychowdhury and Jindal [24]. The results showed that the accuracy in predicting the response of the footing depends heavily on the parameters selection: both the soil and the footing's geometric characteristics. The SSI was concluded to worsen the performance of structural members of ideal RC bare-frame configurations in Behnamfar and Banizadeh [25]. The mid- and the high-rise buildings were the most affected.

The exhaustive modelling of the soil can be based on a direct or a substructure method. In this case, the direct approach has been used. This determines the response of the soil and the structure simultaneously in a single step, providing faster and simpler analyses [26]. It presents several unique features: the soil and the structure can be discretised by finite-element models, the boundaries must receive special treatment, the stress in the soil can be computed easily and 3D nonlinear analysis is possible. The substructure method divides the SSI problem into a series of simpler problems following superposed steps. It leads to more complex analyses as different aspects should be borne in mind (one-dimensional solutions of the site response problem, kinematic interaction problems, coupled soil-structure system among others). Further information of each method can be found in Maslenikov et al. [27]. The direct modelling of the soil is achieved by using finite and boundary elements methods. The seismic vulnerability of high-rise RC buildings was analysed in Karapetrou et al. [6]. The authors pointed out that the complex nonlinear behaviour of the soil underneath the building might introduce additional translation and rotation effects. Also, they concluded that the linear modelling of the soil might lead to unreliable results. These results were also obtained in Cayci et al. [28]. In this case, the authors created and computed the RC structures automatically, using a large database, but the modelling was not done thoroughly.

It can be observed that there is a need to consider the SSI effects in the seismic analyses of structures [29]. More so if these analyses are nonlinear, which are the type of analyses recommended in buildings' seismic vulnerability assessments. By including the SSI considerations, the seismic vulnerability analyses might become tedious due to the complex procedure needed to define them [3]. Furthermore, there is a lack of studies and guidance in the codes on the SSI assessment. In fact, although the EC8 identifies the structures for which the SSI must be included in engineering practices, it does not specify any guideline for their quantification. Hence, the development of procedures to analyse the SSI problems, which can be simple yet fairly accurate, arises as an opportunity to improve the seismic vulnerability analyses.

Hence, the main scope of this study is to investigate the seismic capacity and vulnerability of RC buildings in the city of Lisbon and the development of fragility curves taking into consideration the SSI effects. These effects have not been considered in this kind of constructions nor this type of soil to date according to the author's knowledge. The goal of this study is to fill in the gap identified regarding the quantification of SSI in the seismic vulnerability of RC buildings as well as providing some first conclusions and rules of thumb for the case study area. This work can provide a scientific database so that simplified or intermediate methods such as the BNWM or the macro-element can be validated (which have been extensively used in SSI problems analyses). The use of these methods is part of a future research work that could be used for a forthcoming comparison. Moreover, this work can provide guidance to civil and structural engineers to practically include the SSI effects in their studies.

Unlike the available works such as [30,31], this paper deals with a real case study building (i.e. real structure and soil characteristics), to perform an exhaustive numerical modelling. Also, nonlinear static analyses have been carried out instead of dynamic to speed the calculations and to prove that SSI can be easily included in seismic vulnerability analyses of existing RC buildings.

This study is focused on different objectives summarised as follows:

i. Proposing a method to practically include the SSI effects in the RC buildings seismic assessment. The state of the art has revealed a lack of guidance and easy-to-follow procedures to include the SSI. To do so, the modelling steps and guidance needed to obtain reliable results are defined.

ii. Proposing a method to thoroughly characterise the soil behaviour. In this case, applied to the type of soil that can be commonly found in Lisbon.
iii. Comparing the SSI affection in a Lisbon RC building considering two of the most common approaches to model the SSI: the BNWM and the direct modelling of soil.
iv. Proposing 3D finite element models (FEM) in OpenSees that aims to reproduce the complex soil nonlinear constitutive law in order to represent as realistically as possible the behaviour of the entire system (soil + foundation + structure). The key points needed to bear in mind when modelling the SSI are pointed out.
v. Determining the SSI effects on RC buildings by means of their seismic safety verification and fragility assessment.
vi. Providing a scientific database to validate simplified or intermediate modelling approaches.

The method proposed in this study is divided into four main parts: the characterisation of the case study building and the soil; the numerical modelling of the superstructure and the SSI; the determination of the parameters of the analyses; and the assessment of the seismic safety and fragility. The procedure followed in this research is schematically shown in Fig. 1.

2. Characterisation of the case study

2.1. Building

Unlike most of the related works, a real case study building has been selected to be analysed in this study. It is located in the neighbourhood of *Alvalade* (Lisbon). A proper characterisation of the buildings in this area was carried out in [9]. It was concluded that 28% of the 2249 buildings identified have an RC structure. Half of them are framed buildings, i.e., they only have RC beams and columns as structural elements. Most of these structures are mid-rise buildings (three to six floors) and present irregularities in height: short columns and soft storey-mechanisms. This is one of the typical irregularities proved to worsen the seismic behaviour of RC buildings [32,33]. Moreover, around 70% of them were constructed between 1950 and 1970, before the 1983 Portuguese seismic code. Therefore, these buildings have not been designed to withstand the earthquakes expected and present typical pre-1970 s constructive characteristics [34]: insufficient longitudinal and transversal rebar ratio, smooth rebars, very slender RC columns sections and low quality structural materials [35].

The building selected is one of the most representative RC framed buildings of the area. This configuration can also be found in neighbourhoods around the historic centre of Lisbon (Fig. 2). This building was constructed in the 1960 s. It has five storeys (17.0 m in total) and one storey beneath the surface. The height between floors is irregular. In fact, it presents short columns on the first floor. In plan, the building is symmetrical. On the ground floor, most of the strong axis of the columns are oriented in the X direction. On the rest of the floors, half of them are oriented in the Y direction. On the ground floor, it has a soft storey. Although the building presents RC walls, these are just located at the basement of the building. Therefore, it can be assumed that the structural system is framed rather than wall-framed.

The structural elements' characteristics are listed in Table 1. The dimensions of the columns vary from 20 × 31 cm to 30 × 40 cm, being mainly located in the perimeter and in the centre of the building, respectively. In the case of the beams, they range from 20 × 40 cm to 20 × 60 cm. The characteristics have been expressed as ranging values owing to the variety of RC frames identified in the blueprints. The dimension of the footings is 1.20 × 1.20 × 0.80 m. As can be observed in Fig. 2, some inner shallow foundations are isolated, only the centre ones being connected. This feature has been identified in some buildings in the area by checking the available blueprints from local archives.

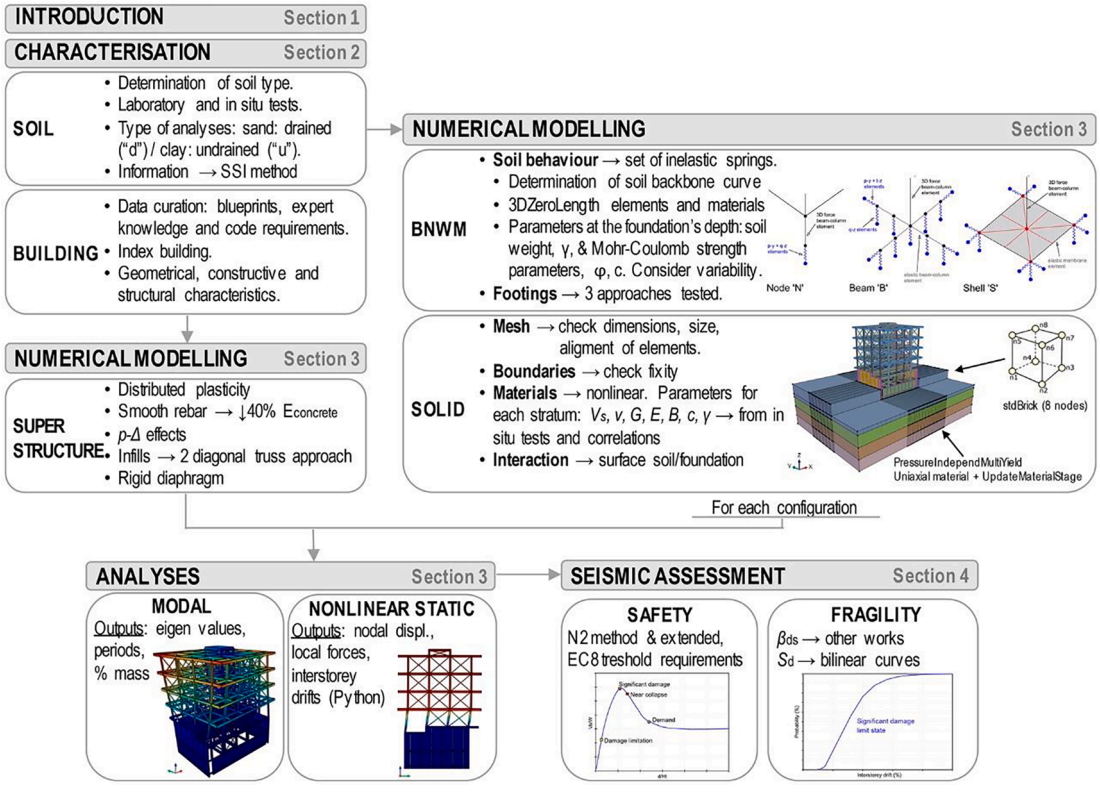

Fig. 1. Flowchart of the method followed in this work.

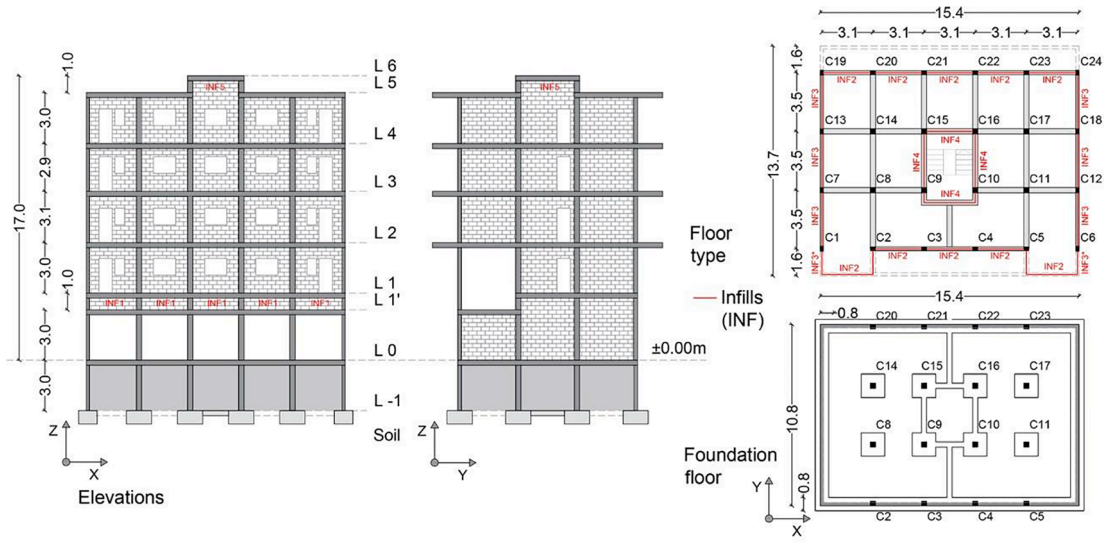

Fig. 2. Schematic configuration of the case study building. Note: 'C' refers to the columns, including a number to label them. 'L' refers to the level. The characteristics of the building are shown in Fig. 7.

Table 1
Building's structural elements' characteristics. Note: the RC walls are located at the basement of the building.

	Columns	Beams	Walls
Dimensions (cm)	20 × 31–30 × 40	20 × 40–20 × 60	
Longitudinal rebar (cm^2)	5.31–38.79	Top: 5.63–16.46 Bottom: 1.42–11.10	3.41–2.45
Transversal rebar (cm^2)	1.58	2.11–2.47	
Thickness (cm)			20

2.2. Soil

In order to properly model the soil behaviour, a thorough characterisation of its properties has been carried out. This has been done based on the geotechnical investigations conducted by [36] and [37]. The soils characterised considering the works of [36] and [37] have been named as soil Type 1 and Type 2, respectively.

In the first work, the geotechnical prospecting was carried out in the area of *Alvalade*, among other Lisbon areas. Information from a total of 6 boreholes (BH) (Fig. 3) and 42 mechanical tests on samples was gathered. The results of these tests indicate that *Alvalade* is characterised by the presence of *Argilas do Forno do Tijolo* up to 20 m in depth, which corresponds to the information available in the Geological Map of the Lisbon Municipality [38]. The granulometric analyses reveal that the soil is composed of 38% clay, 44% silt and 18% sand. It is also concluded that the soil is very homogeneous in depth. It can be classified as silty clays according to the Ferret's Triangle for fine particle sized soils and as 'ClM', medium plasticity clays, according to the UNE-EN ISO 14688-2 [39]. The Atterberg limits tests have also shown that the clay presents high consistency indexes (Table 2). These characteristics are typical for rigid soils. The water table was measured at an approximate depth of 10 m below the ground surface. This soil is identified as soil type 1. According to the EC8-1 classification, both soil types can be classified as type C.

Since the soil is clayey, the analyses have been carried out under undrained conditions, which is the most restrictive situation for this soil. This is due to the fact that when a saturated clay is loaded, it will not let the water drain immediately, remaining undrained, reducing the shear strength as well as the safety coefficient of the foundation. Therefore, it is necessary to assess the short-term stability, in terms of total stresses, which is normally much critical than the long-term stability. For undrained loading, the failure envelope in terms of total stresses is quasi horizontal ($\phi = \phi_u = 0$). Hence, only one parameter is needed, the undrained shear strength (c_u), while the unconsolidated angle of repose (ϕ_u) is 0. The undrained shear strength can be derived from an unconfined compression test, UU triaxial or direct shear tests. The Mohr-Coulomb strength parameters were determined from direct shear and triaxial tests done with the samples (42).

The results have shown that these values do not vary considerably with depth. However, a variability in function of the depth has been identified. Hence, the maximum, medium and minimum values for the unit weight (γ) and c_u have been listed in Table 3. The values have been determined for a depth (z) of 3.80 m, which is the depth of the foundations. These values will be later used in the numerical analyses described in Section 3.2.1.

The shear wave velocity (V_s) and the Poisson ratio (ν) are two of the most important parameters to numerically model the soil. The values of V_s and the compressional wave velocity (V_p) have been obtained following the SPT-Uphole method. This is based on performing standard penetration tests and using the impact energy of the split spoon sampler in the SPT test as a source [40]. ν has been obtained from the results of triaxial and direct shear tests considering different samples listed in the research work referred to. Based on the available experimental tests, an interpretation of the soil layering at the site in terms of V_s and ν is shown in Fig. 4 (a) and (b). Additionally, the compressional wave velocity (V_p) (Fig. 4(c)) has been obtained according to experimental tests and a well-known equation (Eq. (1)). This has been done in order to check whether the values of V_s and ν can be assumed as coherent. As observed in Fig. 4 (c), this comparison validates the values of V_s and ν. From Fig. 4 (a), it can be seen that V_s linearly increases until a depth of around 7.00 m. Then, the values remain approximately constant in depth. This also happens to ν. Nevertheless, in this case, it decreases up to 7.00 m in depth. The medium values of V_s and ν have been used in order to define the constitute law of the soil.

$$\nu = \frac{1}{2}\frac{(V_p/V_s)^2 - 2}{(V_p/V_s)^2 - 1} \quad (1)$$

The experimental tests (triaxial, direct shear, oedometric and compression tests) reveal information regarding the shear modulus (G) (Fig. 5(a)) and the elastic modulus (E) (Fig. 5(b)). The values of these moduli were listed in the research work referred to. Those results have been compared to the values obtained considering widely used geotechnical equations in order to validate them (Eq. (2) and (3)). No information is available regarding the bulk modulus (B). Hence, this is

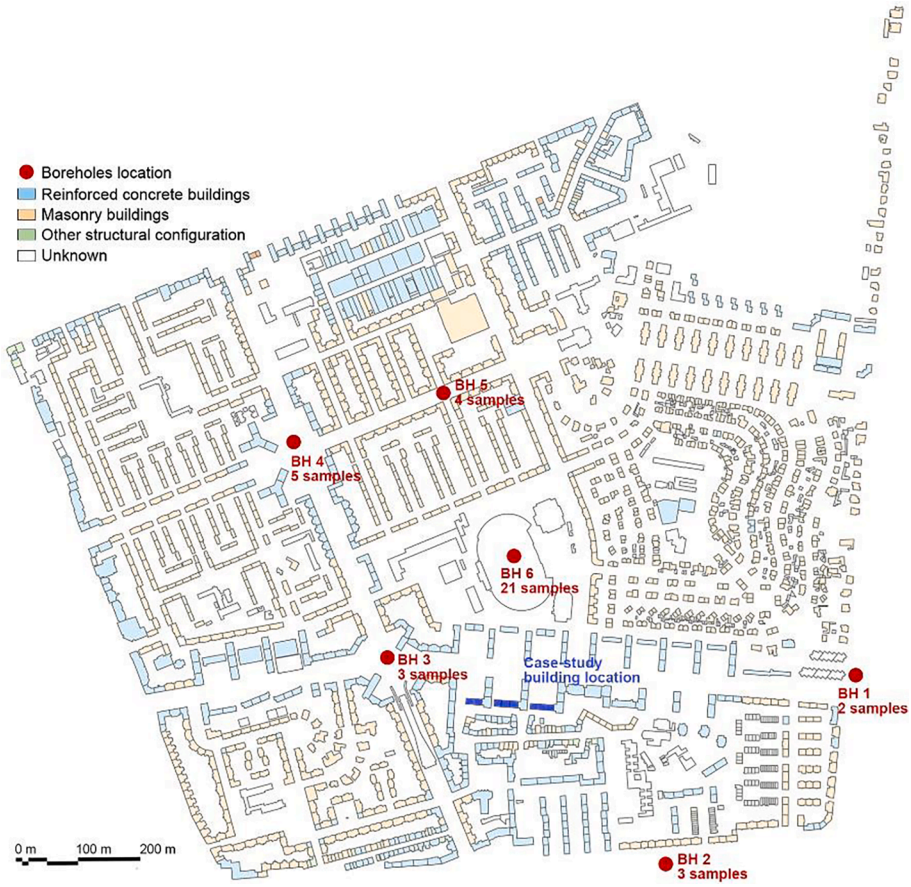

Fig. 3. Location of the boreholes (including the number of samples analysed) and identification of the structural configuration of the buildings in *Alvalade*.

Table 2
Median Atterberg's and consistency limits.

Parameter	*LL* (%)	*PL* (%)	*PI* (%)	*w* (%)	I_C (%)
Argilas do Forno do Tijolo	36.92	21.24	15.71	19.26	1.12

Where: liquid limit (*LL*), plastic limit (*LL*), Plasticity Index (*IP*), humidity, (*w*) and consistency index (I_C).

Table 3
Variability in the soil parameters for the soil type 1.

Soil	Condition	γ (kN/m^3)	c_u (kPa)
Argilas forno do tijolo	Minimum	17.56	$c_{u,min} = 7.23z + 81.24 = 87$
	Maximum	21.7	$c_{u,max} = 17.90z + 201 = 215.3$
	Median	20.14	151.17

obtained from another common equation (Eq. (4)). In this case, two verifications have been carried out considering the value of *E* (Fig. 5(c)) from: experimental tests and the equation. As can be observed, the values of *G* and *E* are similar to those obtained with the equations. In the case of *B*, the values obtained from the experimental tests *E* will be considered in the analyses. From depth 6.00 m onwards, *G* and *E* remain almost constant. In the shallow layers, *G* and *E* increase linearly with depth. *B* equals 2,500 MPa on the surface and increases linearly to remain constant up to a depth of 3.50 m. As previously defined, the soil density (ρ) can be assumed to be constant with depth. According to the information available, a value of 1.79 ton/m^3 has been selected. The comparison between the experimental values from the research work cited and values obtained from the equations has been plotted in Fig. 5.

$$G = \rho V_s^2 \tag{2}$$

$$E = 2G(1+v) \tag{3}$$

$$B = E/3(1-2v) \tag{4}$$

The second work only gathered information from geotechnical prospecting. Those tests were carried out in the neighbourhood of *Entrecampos*, next to the west side of *Alvalade* and near the case study building. The results showed that this area is characterised by the presence of *Argilas do Forno do Tijolo*, the same as the results from the first work. However, the results of the tests reveal that this soil is softer than the first one. It has been identified as soil Type 2. Among other in situ tests, SPTs were performed. There are several equations to obtain V_s considering N_{spt} [41]. In this case, the Imai approach (Eq. (5)) has been used, since it is the most common one.

$$V_s = 91 N_{spt}^{0.317} \tag{5}$$

As shown in Fig. 6(a), the values of V_s are lower than the ones obtained in the previous work. This leads to lower values of *G* (Fig. 6(b)), *E* (Fig. 6(c)) and *B* (Fig. 6(d)). This results in a softer soil than the one previously characterised. In this case, *G*, *E* and *B* have been obtained from Eq. (2), (3) and (4), respectively. Both type of soils will be considered in the 3D finite element models. In this case, according to the available information, ρ has been considered as 1.75 t/m^3.

3. Numerical modelling

The numerical modelling of the structure, the foundation and the soil has been carried out with the OpenSees FEM software [42]. A pre/post-processor has been used to help visualising the geometry and the results

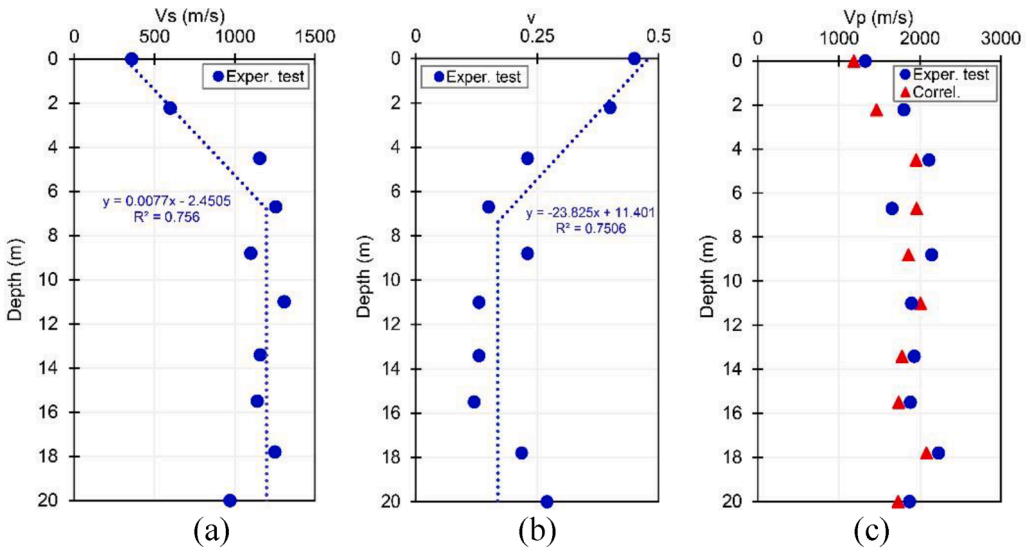

Fig. 4. V_s (a), ν (b) and V_p (c) values obtained from experimental tests and equations for the soil type 1.

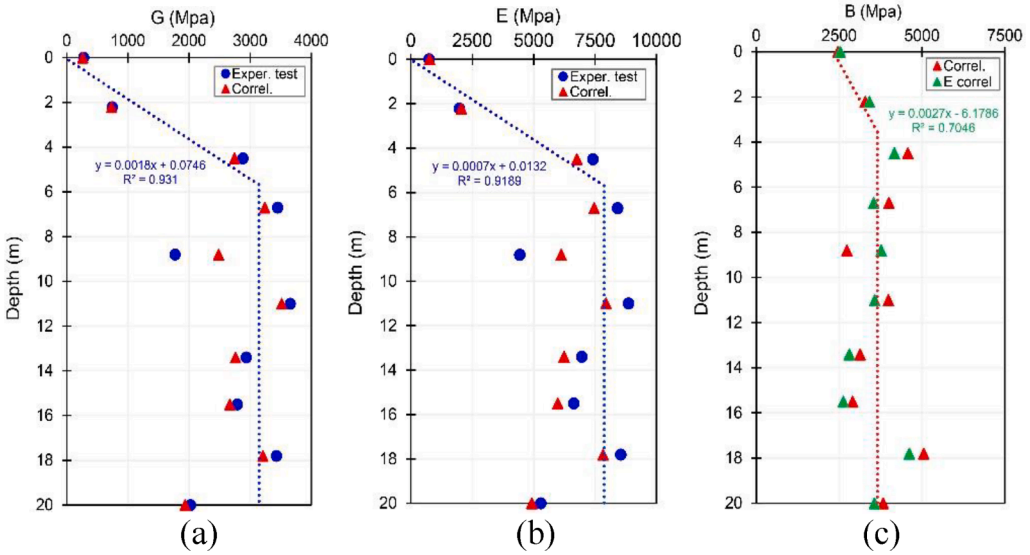

Fig. 5. *G* (a), *E* (b) and *B* (c) values obtained from the experimental tests and equations for the soil Type 1.

of the analyses named STKO [43]. Note that the OpenSees's commands are written within quotation marks to distinguish them from their description.

3.1. Superstructure

There are different options to model nonlinear RC frames, such as the concentrated and the distributed plasticity approaches. The former assumes that the nonlinearity occurs at the end of the frame through plastic hinges. These depend on the input parameters (geometrical and material properties as well as the loading conditions). Therefore, they should be carefully assessed. In this work, the latter approach has been followed as in [9–11]. The distributed approach computes the propagation of plasticity along the length of the elements. Contrary to the concentrated approach, this does not require the calibration of additional plastic elements [44].

'ForceBeamColumn' elements have been used to bear in mind the nonlinear behaviour of the RC frames as well as the p-delta (p-Δ) effects. This constructs a nonlinear frame element object based on the iterative force-based formulation to distribute the plasticity and the plastic hinges along the element. The elements have been discretised into 5 Lobatto integrations. The cross-section of this element has been represented by a fibre section, subdivided into quadrilateral fibres. Each fibre is associated with uniaxial materials where the stress–strain relationship of concrete and steel has been defined. Concrete has been simulated by using the 'Concrete01′ uniaxial material, which takes into account the degradation of the strength in compression with degraded stiffness. To consider the confined concrete in the core, the strength and the strain have been increased in accordance with [45]. In the case of steel, 'Steel02′ uniaxial material has been used, which properly defines its elastoplastic behaviour. In order to take into consideration the effects of smooth rebar, the experimental work on the bond-slip deformations between the concrete and the reinforcing bars has been followed [46]. It was concluded that for the case study building, the smooth rebar effects can be computed by decreasing the elastic modulus of the reinforcing steel by up to 40% as well as the maximum strength. The effect of the staircases has been considered by adding additional distributed loads along the beams that support them. Table 4 lists the structural parameters needed to define each of the uniaxial materials to simulate the concrete, the steel and the infills.

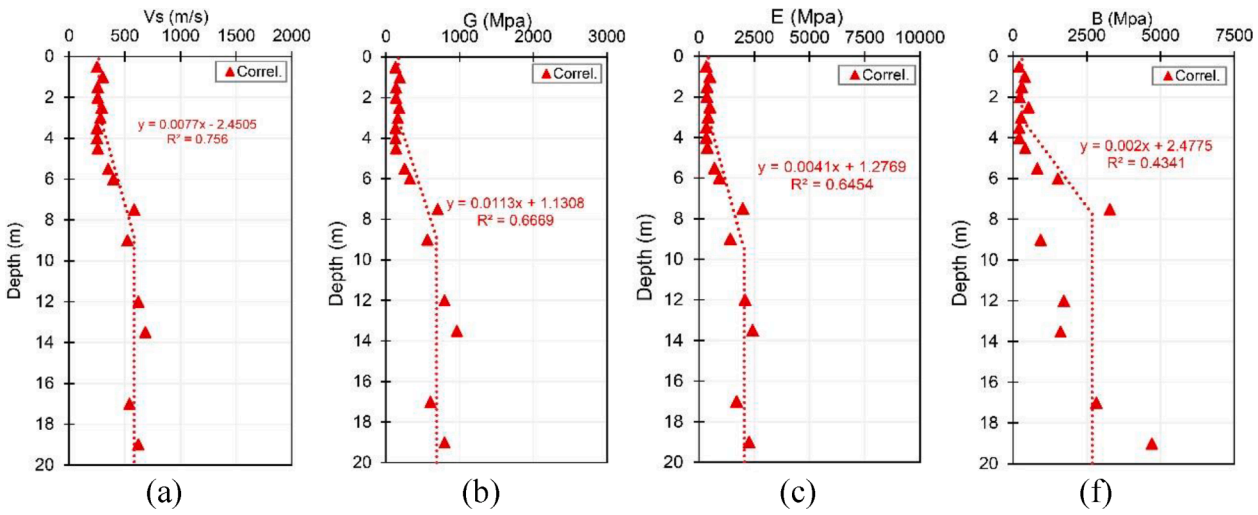

Fig. 6. V_s (a), G (b), E(c) and B (d) values obtained from equations for the soil Type 2.

Table 4
Structural parameters.

Concrete		Steel		Infills	
f_c (MPa)	28	f_y (MPa)	370	G_w (GPa)	1.240
f_{cu} (MPa)	4	E_s (GPa)	310	α	0.05
ε_c (%)	0.002			τ_{cr} (MPa)	0.28
ε_{cu} (%)	0.04			E_w (GPa)	4.092

Where: concrete compressive (f_c) and crushing strength (f_{cu}); concrete strain at maximum (ε_c) and ultimate strength (ε_{cu}); steel yielding strength (f_y); steel modulus of elasticity (E_s); infills shear modulus (G_w); post-capping degrading branch coefficient (α); shear cracking stress (τ_{cr}); masonry elasticity modulus (E_w).

The infills have been modelled by using the two-diagonal truss approach presented in Celarec et al. [47]. It is important to highlight that this OpenSees element has only 3 degrees of freedom (DOF). Therefore, the trusses have been linked to the structure by applying the 'EqualDOF' constraint (constraining X, Y and Z) to the interaction. Uniaxial hysteretic materials have been used to define each branch of the quadrilinear force–displacement relationship of the trusses (Fig. 7). The infills have been grouped in five types according to their similar

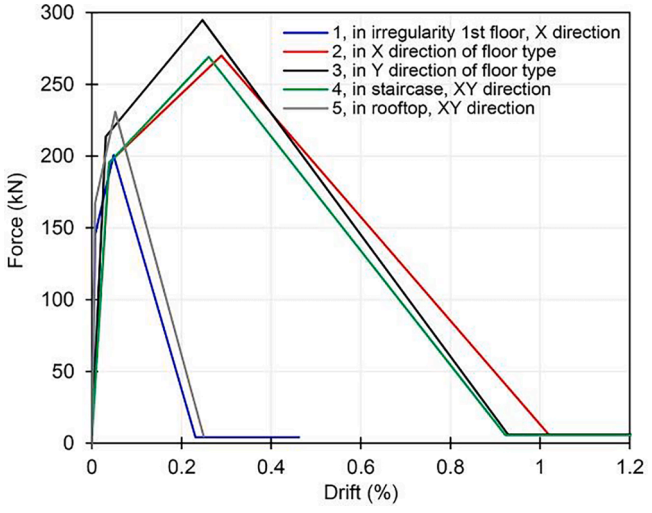

Fig. 7. Quadrilinear force–displacement relationship of the diagonal trusses (in compression), measured in the horizontal direction. The localisation of the infills can be observed in Fig. 2.

constitutive laws. The third branch of the envelope is the post-capping degrading branch, which depends on the elastic stiffness and the parameter α. As stated in Celarec et al. [47], there is a lack of data regarding the estimation of this parameter. In this work, a value of 0.05 has been selected following the recommendations of the referenced work. The influence of the openings has been taken into account by reducing the initial stiffness of the infills by λ_0 as considered in Dolšek and Fajfar [48]. This approach does not distinguish between the type of opening (door or window). Following these authors' suggestions, the strength of the infills has been reduced by 50% only in the case of the doors.

The effects of the rigid slabs have been considered by applying the rigid diaphragm constraint to the node-to-node interaction. This links each floor master node (in the centre of the slab) to the slaves (beam-column joints). Masses have been applied to each structural element according to the gravity loads and the elements' self-weights. The masses of each floor are listed in Table 5. The gravitational loads have been applied to the elements (beams and columns). These have been divided into dead and live loads. The dead loads have included the RC elements and the infills' self-weights and the constructive elements' weights. The live loads have been defined in accordance with the EC8-1.

3.2. Soil-structure interaction

Two approaches have been simulated to take into account the effects of the soil: the BNWM and the direct modelling of soil (as solid).

3.2.1. Beam on nonlinear Winkler method

In this study, three approaches based on the BNWM have been modelled (Fig. 8). In the first approach (Fig. 8(a)), the nodes at the base of the superstructure have been duplicated. A node-to-node interaction has been created to which the soil characteristics have been applied. The foundation is not specifically modelled. The second approach (Fig. 8(b)) is based on modelling the footings with elastic beams. The 'Elastic' physical property and the 'elasticBeamColumn' elements have been applied to the beams. The third approach (Fig. 8(c)) is based on modelling the footings with shells. The 'ElasticMembranePlateSection' physical property and the 'ShellMITC4' element have been applied to the faces modelled.

In order to model the soil behaviour, nonlinear springs have been added in different directions. The horizontal springs are called *p-y* and *t-z* while the verticals are *q-z*. The materials and the models have been validated by means of centrifuge tests [49]. In OpenSees, the *p-y*, *t-z* and *q-z* springs proposed to simulate the soil behaviour can be modelled as uniaxial materials named 'PySimple', 'TzSimple1' and 'QzSimple1',

Table 5
Masses of each floor.

Floor	−1	0	1′	1	2	3	4	5	6	Total
Mass (ton)	187.26	215.28	73.21	199.32	311.96	308.77	311.64	266.80	13.94	1608.11

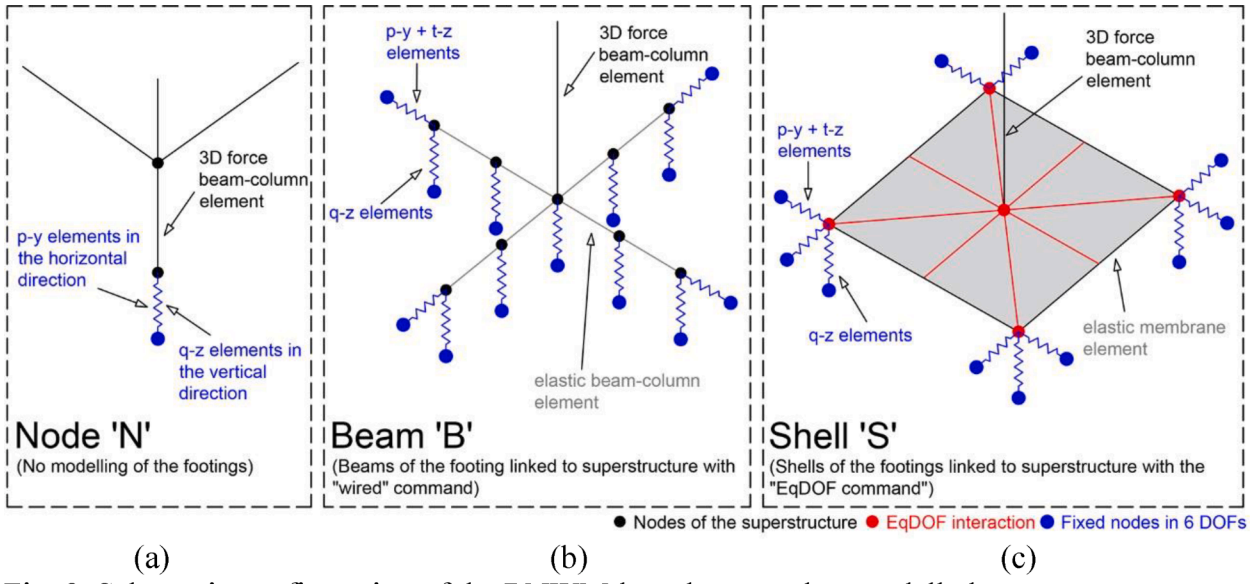

Fig. 8. Schematic configuration of the BNWM-based approaches modelled.

respectively. These materials are later applied to the direction considered by using the 'zerolengthMaterial' according to Fig. 8. Then, 'zeroLength' elements have been applied to distribute the material in 3D along the interaction. The behaviour of these materials is presented as a backbone curve with an initial elastic behaviour ending in a soft nonlinear behaviour (Fig. 9). The curve is described according to the ultimate capacity (lateral or bearing) and the displacement at which 50% of the load is mobilised. In the case of the 50% displacement, this is obtained considering the ultimate capacity and the spring stiffness (K), modified by a j-factor. This factor depends on the soil and the type of springs. It is defined in the OpenSees documentation (Table 6). The unloading stiffness of the springs (k_{unl}) is considered equal to the initial one as concluded in [50]. The stiffness of the springs has been calculated according to Gazetas's equations [51]. These *formulae* depend on the geometric and the structural characteristics of the footings.

P-y springs simulate the passive horizontal pressure based on Rankine's theory where p_{ult} is the passive earth pressure (Eq. (6)). This depends on the soil weight, the depth of the footing (D_f) and K_{py}. In this case, K_{py} is the passive earth coefficient calculated based on the Coulomb theory (Eq. (7)). y_{50} represents the displacement at which 50% of p_{ult} is mobilised (Eq. (8)).

Table 6
Values of j-factor to define y_{50} and z_{50} according to the soil type.

	Clay	Sand
j_{qz}	0.525	1.39
j_{py}	8.00	0.524
j_{tz}	0.708	2.05

$$p_{ult} = 0.5\gamma K_{py} D_f^2 \tag{6}$$

$$K_{py} = \tan^2\left(45 + E\sqrt{2}\right) \tag{7}$$

$$y_{50} = j_{py}\frac{p_{ult}}{K_{py}} \tag{8}$$

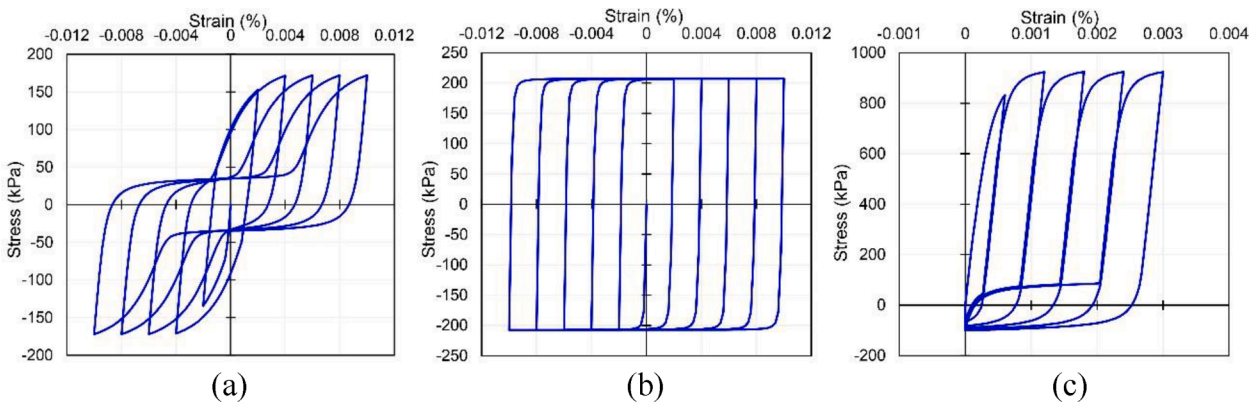

Fig. 9. Material behaviour of the *p-y* (a), *t-z* (b) and *q-z* (c) nonlinear springs considering the medium values of the soil parameters from Table 3.

T-z springs capture the slippage of the foundation on the soil. The *formulae* are based on the Mohr Coulomb failure criterion and Rankine's theory. t_{ult} (Eq. (9)) is the frictional resistance pressure which depends on the vertical load at the surface of the footing (W_g), the frictional angle between the soil and the footing (δ), the area of the footing (A_b) and the cohesion (c). δ varies from $\phi/3$ to $2\phi/3$ according to the foundation's constructive procedure. In the construction of shallow footings, the concrete is poured onto the soil directly without using a formwork. Therefore, δ is equal to $2\phi/3$. Different values of W_g have been obtained according to the position of the footing: corner, middle and centre. Therefore, different values of t_{ult} and z_{50} have been determined according to the geometry and the loads. z_{50} is the displacement at 50% of t_{ult}. In order to determine the spring's stiffness, K_h, Gazetas's equations for the horizontal (h) translation axis have been used. In this case, the footings are squared, therefore, the general formulation has been considered (Eq. (11)). If the footings are rectangular, both *formulae* should be used according to their dimensions (including Eq. (12)) and therefore different values of z_{50} should be calculated.

$$t_{ult} = W_g \tan\delta + A_b c \tag{9}$$

$$z_{50} = j_{tz}\frac{t_{ult}}{K_{x,y}} \tag{10}$$

$$K_{h(x,y)-towardslongside} = \frac{GL}{2-\nu}\left[2+2.5\left(\frac{B}{L}\right)^{0.85}\right] \tag{11}$$

$$K_{h(x,y)-towardsshortside} = \frac{GL}{2-\nu}\left[2+2.5\left(\frac{B}{L}\right)^{0.85}\right] + \frac{GL}{0.75-\nu}\left[0.1\left(1-\frac{B}{L}\right)\right] \tag{12}$$

Where: B and L correspond to the short and long dimension of the footing, respectively. G and ν are the concrete shear modulus and the Poisson ratio of the footing, respectively.

Q-z springs capture the sinking and the detaching behaviour of the soil. q_{ult} is the ultimate bearing capacity and this can be calculated using the general *formulae* developed by Terzaghi. In this case, the shape of the footings (s), the depth (d) and the load inclination (i) factors have been also considered apart from the bearing capacity factors (N). q_{ult} has been calculated following the *formulae* developed by Meyerhof and Brinchen-Hansen (Eq. (13)). In the *formulae*, the variables with subscript c refer to the cohesion; q to the earth pressure at the footing depth; and γ to the soil unit weight. q_{ult} is affected by the position of the footing (corner, middle and centre). However, in this case, no differences have been found in the values of the horizontal loads and the moments from the gravitational analyses. Therefore, only one type of *q-z* spring has been considered. In order to define z_{50}, the displacement corresponding to 50% of q_{ult}, the stiffness at the vertical (z) translation, K_z, has been calculated using Gazetas's equation (Eq. (15)).

$$q_{ult} = cN_c s_c d_c i_c + \gamma D_f N_q s_q d_q i_q + 0.5\gamma B N_\gamma s_\gamma d_\gamma i_\gamma \tag{13}$$

$$z_{50} = j_{qz}\frac{q_{ult}}{K_z} \tag{14}$$

$$K_z = \frac{GL}{1-\nu}\left[0.73+1.54\left(\frac{B}{L}\right)^{0.75}\right] \tag{15}$$

3.2.2. Direct model of soil

The adjacent soil of the building has been modelled with a mesh of 48x33x20 m (X, Y and Z). In order to define a proper mesh, three points need to be considered: i) the dimensions of the volume; ii) the mesh size and type; and iii) the alignments of the elements. There are several works on the definition of the mesh dimensions [21]. In this case, the common approach based on modelling the mesh according to the length of the building in each direction has been used [52]. It has been proved that this approach guaranties that the displacements at the boundaries do not affect the superstructure. It is known that coarse meshes do not capture the behaviour of the soil properly since it tends to behave as rigid. By contrast, very refined meshes produce similar results to the optimal mesh but the computing effort is notably increased. In this work, the procedure suggested by the STKO developers on the mesh size has been followed. Later, a sensitivity analysis has been carried out on the mesh size to check the consistency of the results.

In this case, in order to define the mesh of the model, the common approach considering the dynamic characteristics of the soil and the structure has been followed. According to the STKO manual, the minimum value of V_s has been divided by the frequency of the soil domain and a predefined number of elements. To properly calculate the footings displacement, the mesh has been refined near the footing edges where a high stress gradient may occur. The solid elements have been modelled with the 'Structured' algorithm and the 'Quad/Hexa' typology. Also, the links and interactions need to be aligned, otherwise the results will not be accurate. The 3D FEM proposed tends to reproduce the soil nonlinear constitutive law to realistically represent the behaviour of the entire system (soil + foundation + structure) (Fig. 10).

Brick elements are defined in OpenSees to capture the soil small deformations. In OpenSees, it is possible to perform analyses on two-phase saturated soil (multi-phase). However, in this work, the analyses have been performed under undrained conditions (single-phase) since it is the most restrictive condition for the case study type of soil. Eight-node hexahedral elements have been applied to the soil volume named 'SSPbrick' (Fig. 11). These elements enable performing faster analyses since they generate single-point integrations instead of full integrations. The mesh is composed of 31 837 nodes and 31 837 brick elements. The lateral boundaries have been fixed in the X and Y directions, respectively. The nodes at the base have been fixed in all directions

The soil constitutive model has been defined by using the 'PressureIndependMultiYield' (PIMY) material. This is an elasto-plastic material that aims to characterise the soil's nonlinear stress–strain response. It was first developed by the UC San Diego, which has implemented different soil models in OpenSees [54]. The PIMY material is based on the Von Mises multisurface-plasticity theory for cyclic hysteretic response to control the shear strain accumulations (Fig. 11) [53]. It has been implemented in OpenSees to simulate elasto-plastic undrained clay-type shear response since this type of soils are insensitive to the confinement change (pressure independent materials).

According to the soil characterisation, three layers have been defined to capture the soil behaviour in line with the depth. The materials have been applied to the soil bricks. The 'UpdateMaterialStage' command has

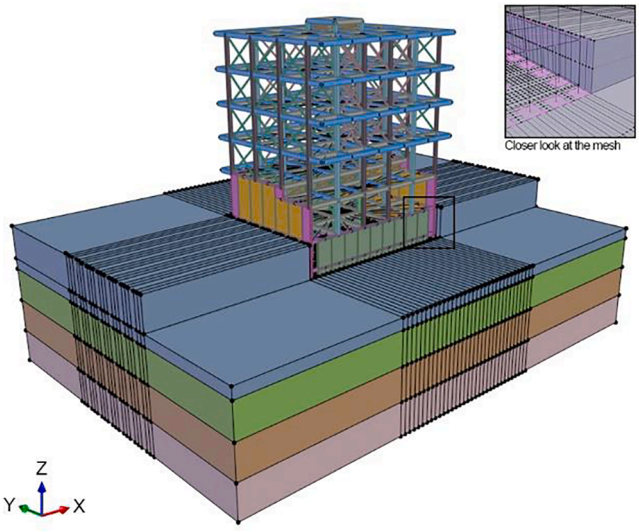

Fig. 10. 3D modelling of the entire system: soil + foundation + structure.

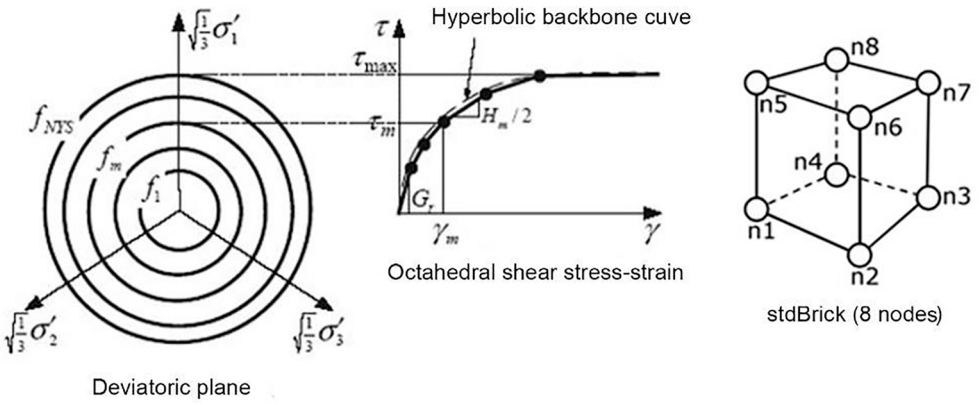

Fig. 11. 'PressureIndependMultiYield' soil material's failure criterion [53].

been used so that the soil behaves as plastic. Non-convergence problems may arise if the behaviour of the soil is updated after this analysis: the soil turns suddenly into nonlinear, but it might not manage to bring the elastic stress into the yield surface all at once. This is due to the fact that during the effect of the gravitational loads, stresses might be generated outside its linear limit. This might happen in buildings with considerable gravitational loads. Therefore, this command has been implemented before the gravitational analyses start.

The footings have been modelled as solids and the 'SSPbrick' elements have been applied to the volumes. The 'beamSolidCoupling' command has been used to link the superstructure base-nodes with the superficial face of the footings' solids. 'EqDOF' constraints have been

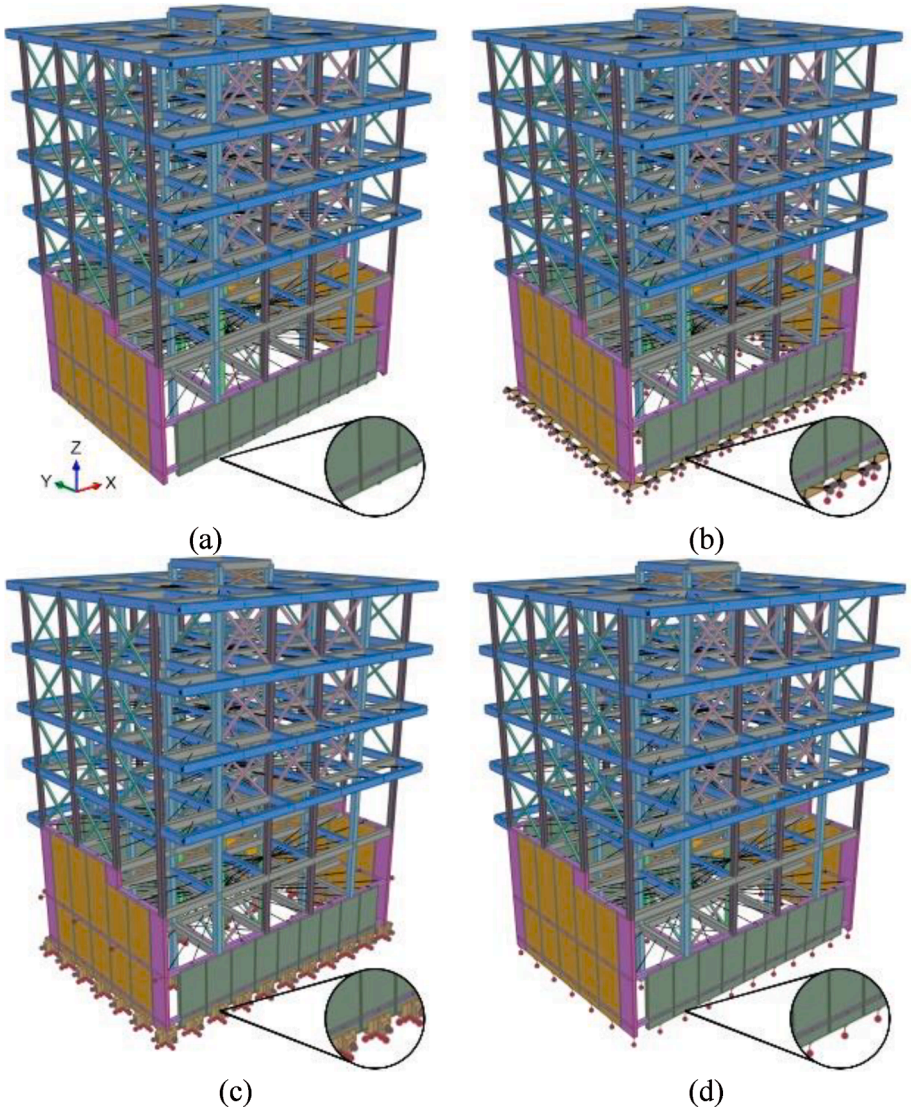

Fig. 12. 3D representations of the FB (a), WMS (b), WMB (c) and WMN (d).

applied to link the soil and the footings' surfaces. This type of constraints generates a multi-point constraint between nodes.

3.3. Models analysed

The models considering the SSI effects have been compared to the fixed-base model (FB). The nodes at the base of the FB models have been fixed in the 6 DOFs: X, Y, Z, R_x, R_y and R_z. The models considering the SSI effects based on the BNWM are named as 'WM' followed by the type of approach definition: node (N), beam (B) and shell (S). A 3D representation of the models is shown in Fig. 12. According to the soil characterisation, three soil configurations have been modelled for the BNWM models considering the maximum (A), medium (B) and minimum (C) values of the soil parameters for the undrained situation (Table 7).

The models with a 3D modelling of the soil have been defined as 'CS' followed by the type of soil considered, as defined in Section 2.2: Type 1 from [36] (CS1) and Type 2 (softer) (CS2) from [37]. For these models, the soil and the foundation body forces have been applied as 'VolumeForces' and they have been added to the gravitational load pattern. Thus, these loads are applied incrementally to avoid convergence problems. The soil and the layer characteristics considered in the analyses are listed in Table 8. Since the analyses are considered under undrained conditions, ϕ_u and d, the constant variation of G and B for the initial effective confinement (ϕ_i'), are equal to 0. These change only under drained conditions. The reference means that the effective confining pressure at maximum values of ρ, G and B (σ_r) is equal in all the cases since it is related to the characteristics of the laboratory tests. The masses have been applied to the solids as 'VolumeMass'.

3.4. Nonlinear static analyses

Despite the fact that dynamic analyses are widely used in seismic vulnerability analyses, only nonlinear static analyses have been carried out in this work. This is due to that the goal of this paper is to speed calculations and to prove that the SSI, which can considerably affect the results, can be easily included in this type of analyses.

The nonlinear static analyses performed have been performed with OpenSees in both orthogonal directions (X and Y) to determine the capacity of the models. Although the EC-8 establishes that at least two load patterns should be considered in this kind of analyses, the results will only reference the modal load pattern since this is the most restrictive. For this load pattern, worse results in terms of seismic strength capacity, and thus seismic performance, have been obtained for all the models compared to the uniform pattern. The analyses have been carried out with the Parallel option, considering the following parameters: 'Penalty' constraint, the 'Mumps' system and the 'Krylov' algorithm. A load-control and a displacement-control integrator have been used in the gravitational and nonlinear static analyses, respectively.

The eigen vectors in each direction for all the master nodes (located in the middle of each slab) have been obtained from the modal analyses. The *-genBandArpack* solver has been used due to the many constraints in the models. Then, a displacement-normalisation has been performed.

The N2-method and its extended version (to take into account the infills' effects) have been used to define the single degree of freedom (SDOF) idealised bilinear curves and the target displacement.

Table 8
Soil and layers characteristics.

Soil type	Layer	Depth (m)	ρ (ton/m^3)	G (MPa)	B (MPa)	c (kPa)	σ_r (kPa)	d
Soil 1	Layer 1	0–6	1.79	3292	4511	50	80	0
	Layer 2	6–12	1.79	3090	967	50	80	0
	Layer 3	12–20	1.79	6090	4496	50	80	0
Soil 2	Layer 1	0–4	1.75	203	339	38	80	0
	Layer 2	4–8	1.75	800	1500	38	80	0
	Layer 3	8–20	1.75	794	4701	38	80	0

4. Seismic safety and fragility assessment

4.1. Seismic safety definition

The seismic safety of the all the models has been assessed by determining the local damage in the structural elements according to the demand/capacity ratio (*DCR*) procedure established in Part 3 of Eurocode 8 (EC8-3) [55]. Therefore, three damage limit states (LS) have been used considering the ductile and brittle failure: damage limitation (DL), significant damage (SD) and near collapse (NC).

For the ductile behaviour, NC LS is assessed by calculating the ultimate chord rotation (θ_{um}). The SD LS is defined by 75% of the θ_{um}. The DL LS is calculated considering the yielding chord rotation (θ_y). Each damage LS has been calculated when the demand chord of one column reaches the capacity values of θ_{um} and θ_y. The brittle failure has been defined according to the shear capacity of the columns (V_R).

In this work, the failure of the structure has been assumed when one of the vertical structural elements (columns) reached the SD LS [56].

A peak ground acceleration (PGA) of 0.15 g (Zone 1.3, Lisbon) [56] and the EC8-1 provisions have been considered to define the elastic response spectrum. This action corresponds to a return period (T_R) of 475 years. Only the Type 1 response spectrum has been used.

4.2. Fragility analyses

The performance of the models is also assessed by means of fragility curves. These define the probability of reaching or exceeding a certain damage state (d_s), considering the spectral displacement (S_d). These curves bear in mind the uncertainties and the variability of the analyses as well as the definition of the seismic demand. In this work, the fragility curves for the FB models have been compared with the SSI models. The curves have been defined according to the well-known lognormal cumulative distribution (Eq. (16).

$$P[d_s|S_d] = \Phi\left[\frac{1}{\beta_{ds}} ln\left(\frac{S_d}{\overline{S}_{d,ds}}\right)\right] \tag{16}$$

There are two main parameters needed in the definition of fragility curves: the logarithmic standard deviation (β_{ds}) and the logarithmic mean standard deviation ($\overline{S}_{d,ds}$,). Both parameters should be defined

Table 7
Values of *p-y*, *t-z* and *q-z* nonlinear springs materials.

Soil	γ	c_u	p_{ult} (kPa)	y_{50} (cm)	q_{ult} (kPa)	z_{50} (cm)	t_{ult} (kPa)			z_{50} (cm)		
Conf.							Corner	Middle	Central	Corner	Middle	Central
A	γ_{max}	$c_{u,max}$	460.59	2.3	1344.53	0.274	331.04	418.03	592.00	0.130	0.164	0.232
B	γ_{med}	$c_{u,med}$	187.62	0.8	948.53	0.242	207.34	285.34	441.34	0.0812	0 0.0112	0 0.173
C	γ_{min}	$c_{u,min}$	90.39	0.4	550.66	0.113	86.28	155.59	394.21	0.0338	0.0061	0.115

according to the characteristics of the buildings under study and considering many models and uncertainties. This is not the goal of this paper, therefore the values of β_{ds} have been defined considering the work developed in [57]. These authors proposed fragility curves for infilled RC buildings in Portugal regarding the construction date, the yielding period and the seismic zone. However, they did not take into account the SSI effects in their analyses. Nevertheless, they can offer a first approach to the fragility performance of these models. Only the values of β_{ds} for the SD LS have been selected, being 0.40 and 0.30 for the X and Y directions, respectively. These have been defined according to the characteristics of the case study building, a mid-code located in the seismic zone B (Lisbon). Since only the values of the SD LS have been borne in mind, for the determination of $S_{d,ds}$ the displacement corresponding to the SD LS previously assessed has been considered.

5. Analysis of the results

5.1. Dynamic characteristics of the numerical models

This section shows the results obtained and discusses them. The periods in the X and Y direction of the most representative models have been shown in Table 9. It is intended to shed some light on the different values that can be obtained if the SSI is considered. However, it should be mentioned that the period of the building with and without the surrounding soil cannot be directly compared. This information can be useful to prove that the SSI has been properly modelled. As expected, it can be observed that increasing the soil flexibility leads to higher periods. Also, for future dynamic analyses, it can be seen that the models could behave considerably differently due to consideration of the masses.

The fundamental modes of vibration for the FB and for the CS1 models are shown in Fig. 13 and Fig. 14, respectively. It can be observed that, although the periods increase, the configuration of the modes of vibration do not differ. The principal modes of vibration are the same for both configurations as well as for the BNWM models. Mode 1 (a) is for the Y direction and Mode 2 (b) for the X direction. Mode 3 (c) is a torsional mode of vibration. Modes of vibration 1 and 2 correspond to more than 60% of the effective mass of vibration. Therefore, torsional effects can be neglected. It can also be observed that in both models, the deformation starts from the irregularities located at the ground floor. Additionally, in Fig. 14, it is shown the interaction between the 3D soil, the foundation, and the superstructure.

5.2. Capacity curves and seismic safety verification

All capacity curves depicted in this work used normalised values, i.e., the base shear force (V_b) and top displacement (d) have been divided by the building's entire weight (W) and height (H_t), respectively. The results have been shown for the equivalent SDOF system. It is worth mentioning that for the BNWM models and the models with direct modelling of the soil, the displacement d is the displacement relative to the base of the structure (i.e. the foundation deflection is substracted to the top horizontal displacement of the building). The analyses were carried out in an Intel Pentium i5 with 16 Gb of RAM and four cores. It took 4 and 180 min to run the analyses of the Winkler method and the direct soil models, respectively.

Table 9
Periods for the X and Y direction.

Model/direction	X	Y
FB	0.53	0.59
CS1	1.49	1.77
CS2	1.48	1.74
WMS_B	0.57	0.66
WMB_B	0.59	0.67
WMN_B	0.69	0.85

In order to check whether the case study building is affected by the p-Δ effects, a comparison between the capacity curves obtained with and without these effects has been evaluated. The models considered to analyse the p-Δ effects have been FB. In Fig. 15, it can be observed that if p-Δ effects are considered, the maximum capacity strength of the models can be reduced by up to 42%. Regarding the displacements corresponding to the maximum strength, they have decreased in the X and Y direction from 0.064 m to 0.044 m and 0.078 m to 0.066 m, respectively. Therefore, due to the geometrical properties of the structural elements of the case study building and the significant vertical loads, the p-Δ effects cannot be omitted in the study.

Figure 16 shows the SDOF capacity curves of the FB and the BNWM models considering the medium values of the soil. The WMS model has obtained similar curves to the model with solid soil and the same soil type. The curves for the WMB are also slightly similar. In this case, footings are modelled but not as thoroughly as in the first approach. Moreover, this configuration needs more modelling time than the WMS. In contrast, the WMN curves are considerably different. This is due to the considerably different initial stiffness, resulting from the lack of modelling of the footings. The damage has only been plotted for the most significant models: FB and WMS. It can be observed that for the WMS, the NC LS occurs in both directions for smaller displacements due to the lower stiffness. Moreover, it can be seen that the ratio between the demand (S_{demand}) and the SD LS ($S_{d,ds}$) displacements is considerably higher for the models with SSI than for the FB models for both directions (Table 10).

Since the WMS has been the configuration with more similar results to the solid models, it has been chosen to assess the variability on the soil parameters. In Fig. 17, the different SDOF WMS capacity curves for each type of soil (A, B, C) have been plotted. It can be observed that the maximum capacity can vary by up to 10% in both directions. However, the curves for the C soil are not as different from the B soil curves as the A soil curves are.

From the analyses considering the BNWM, it has been observed that the ultimate capacities of the soil (p_{ult}, t_{ult} and q_{ult}) are the most important parameters affecting the behaviour of the buildings. Regarding the p-y springs, lower values of p_{ult} lead to higher displacements in the backbone curve and, therefore, in the capacity curve of the buildings. The main parameters affecting p_{ult} are the ϕ and the K_{py}. Also, but to a lesser extent, the γ and the D_f affect it. If these parameters are higher, p_{ult} increases, resulting in a better structural behaviour. The area of the footings and K_{py} are the parameters most affecting y_{50}. These results have been obtained for a simple foundation configuration: shallow footings on a clayey soil for a case-study RC building. However, this could change if the energy dissipation is considered as concluded in [58], or for other type of buildings, with different dynamic characteristics (different fundamental frequencies). Despite this, it should be pointed out that in the work presented in [58], the foundation was composed of groups of piles. The interaction between the soil-foundation and the piles among them leads to more complex analyses. In these cases, the energy dissipation could play an important role in the seismic assessment.

In the case of the t-z springs, higher values of t_{ult} increase the shear forces resisted by the structures. The main parameters affecting t_{ult} are the ϕ and the c, and, to a lesser extent, the area of the footings. Higher values of the Mohr-Coulomb strength parameters result in higher shear forces of the capacity curves. z_{50} does not affect the capacity curves significantly. Regarding the q-z springs, they do not affect the capacity of the structures considerably since these springs are only capturing the sinking of the structures. The main springs capturing the behaviour of the structures are the horizontal p-y and t-z. These springs tend to capture the soil horizontal passive pressure and the slippage of the footings on the soil, which matter in horizontal analyses. It has also been observed that the distance of the interaction of the springs does not affect the behaviour of the structures. In OpenSees, 'zeroLength'

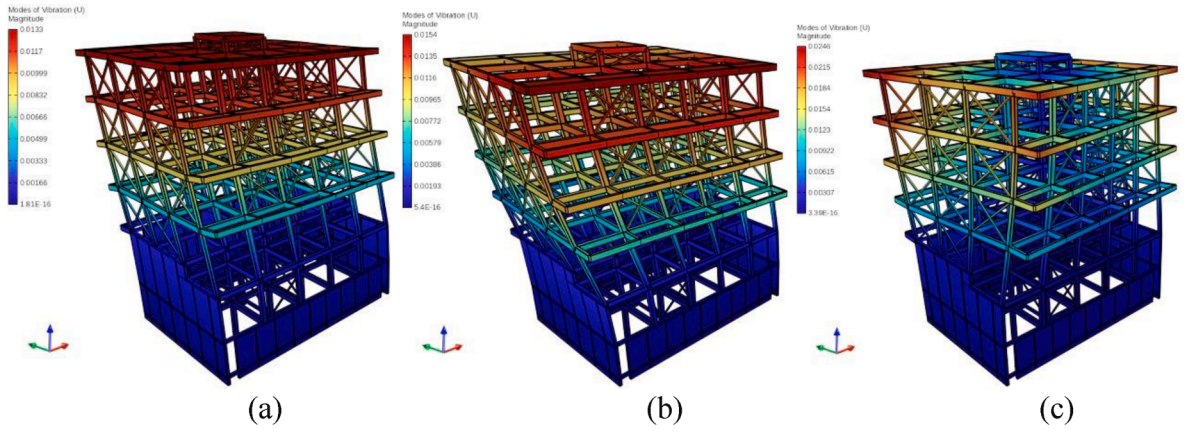

Fig. 13. FB Modes 1 (a), 2 (b) and 3 (c) of vibration.

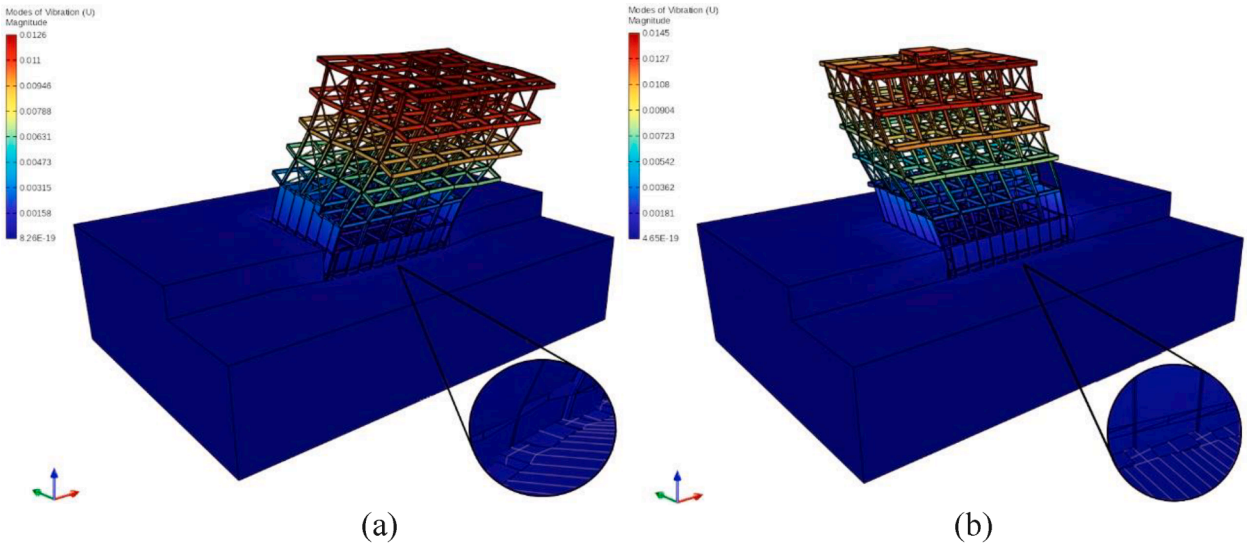

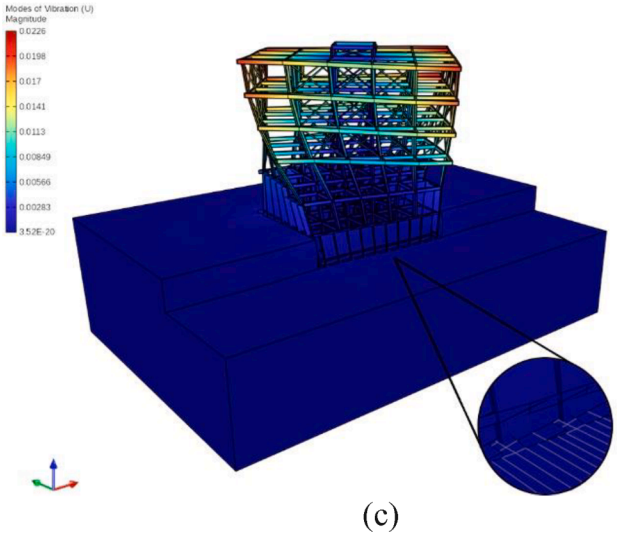

Fig. 14. CS Modes 1 (a), 2 (b) and 3 (c) of vibration.

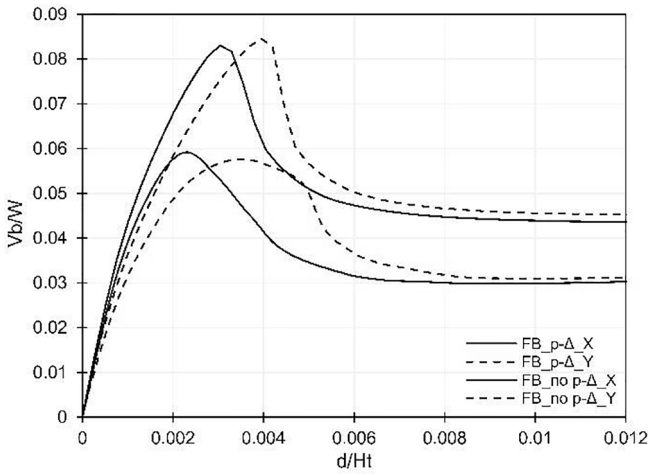

Fig. 15. FB model SDOF capacity curves in the X and Y direction with and without considering the *p-Δ* effects.

elements do not take into account the displacement and the rotation since the software assumes a zero-length finite distance between nodes.

In Fig. 18, the FB SDOF capacity curves have been compared to the curves considering the soil as solid. The reduction of the initial stiffness of the models has not been very high due to the fact that the 3D modelling of the soil depends mainly on V_s. For the case study area, these values are considerably high for all the geotechnical profile, which shows that it is a very rigid soil. It can be observed that the curves for the soil Type 1 decrease by up to 10% in both directions. In the case of the soil Type 2, they decrease by up to 15%. The CS1 curves present higher values of initial stiffness, leading to higher maximum capacities. This is related to the higher soil values of *G* and *B* defined for this soil type than the values for CS2. It has been checked that if the models present coarse meshes, they tend to behave as rigid, as if they were FB. Therefore, as pointed out in [59], refined meshes can lead to reductions in the estimation of the seismic capacity. Also, the results considering the soil as linear, not updating the material stage to behave as plastic, has also been calculated. It has been obtained that the capacity curves are also similar to the FB model. Therefore, as shown in Karapetrou et al. [6], modelling the soil as linear in the seismic vulnerability analyses leads to unreliable results. The reduction of the capacity of the buildings is not as high as the results obtained with the BNWM configurations. As seen in [59], this is due to the lack of properties considered in those configurations, such as: the presence of rigid and deep soil layers; the modelling of footings as solid; the consideration of the complete behaviour of the soil; and the application of interactions to soil-footings surfaces.

As it can be observed in all the capacity curves, the residual strength derived from the RC structural elements remains almost constant in most cases. Therefore, it can be perceived that for this case, the SSI mainly affects the initial stiffness and the maximum strength of the models. In addition, the behaviour and the deformed shape of the building are the same with and without SSI (Fig. 19). However, including SSI effects worsens the results of the analyses. For the RC building case study, the damage is concentrated in columns at the soft storey mechanism in both cases. However, if the SSI are included, the damage in these columns occurs at earlier steps of the analyses (lower values of displacements) due to the increase of the flexibility of the system and the reduction of the maximum strength.

5.3. Fragility curves

In Table 10, the DCR ratio between the S_{demand} and the $S_{d,ds}$ has been calculated for the most significant models. A ratio larger than one means that the model is not complying with the safety requirements established in the EC8-3. It can be seen that none of the models comply with this safety condition. Moreover, if the SSI are included in the analyses, this ratio increases. In the case of solid models, the ratio can increase by up to 30% and 11% in the X and Y direction, respectively, compared to the FB models. For the most representative WNBM configuration, the results are significantly higher due to the different values of stiffness, increasing by up to 51% and 122% in the X and Y direction, respectively.

In Fig. 20, the fragility curves for these configurations are shown considering only the SD LS. This is the LS that needs to be considered in the seismic vulnerability analyses of existing buildings according to the EC8-3 [56]. It can be observed that the probability of having more significant damage increases if the SSI are included. Due to the lower values of $\beta_{ds,\ SD}$ for the Y direction, the probability of SD is higher for smaller displacements. It can be observed that the CS1 curves present 20% more probability of exceedance than the FB models. This percentage rises to 45% for the WMB model.

The local failure of the footings has been checked. The allowable bearing capacity of the soil (q_a) has been calculated considering the

Table 10
Ratio between the S_{demand} and the $S_{d,ds}$.

Model/direction	X	Y
FB	2.23	1.53
CS1	2.70	1.70
CS2	2.90	1.69
WMS_B	3.37	3.40

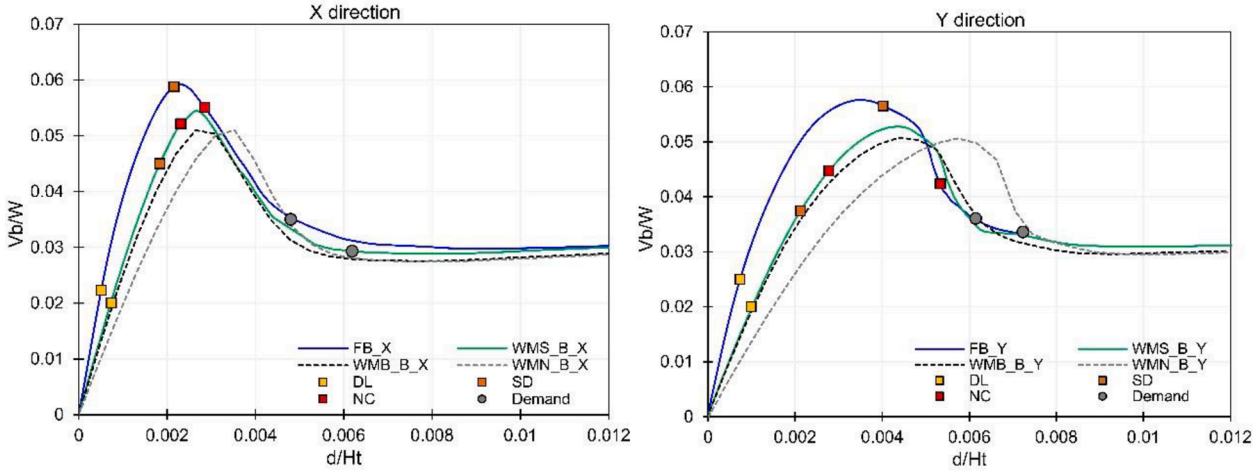

Fig. 16. SDOF capacity curves in the X and Y direction considering different configurations of the BNWM and medium values of soil.

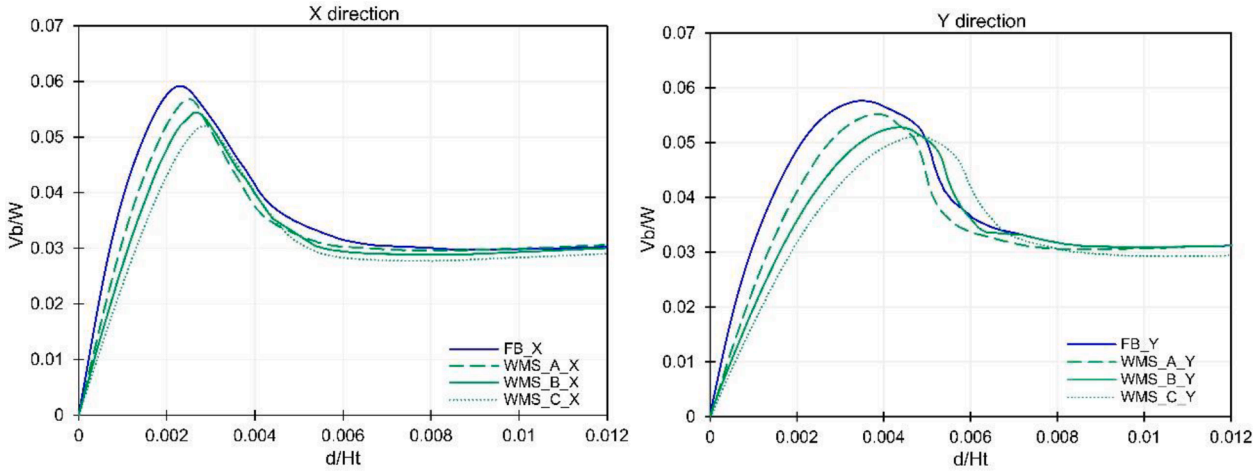

Fig. 17. SDOF capacity curves in the X and Y direction considering the WMS model and the different values of soil.

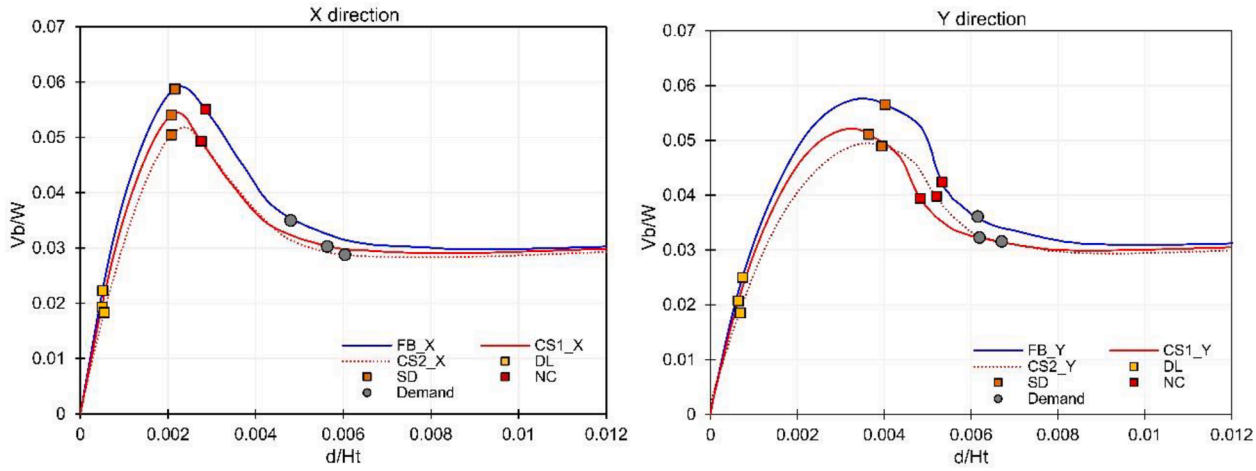

Fig. 18. SDOF capacity curves in the X and Y direction considering different 3D soil models.

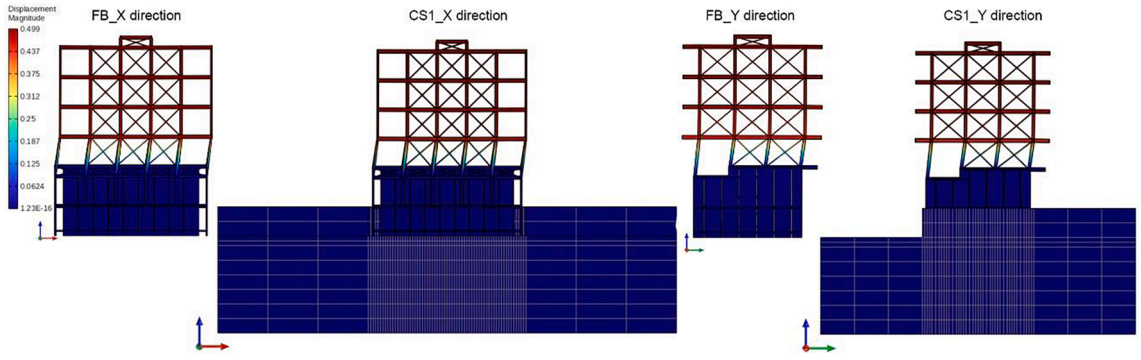

Fig. 19. Deformed from the nonlinear static analyses of the FB and CS1 models.

Brinchen-Hansen formulation (Eq. (13)) for short-term conditions. For this case, q_a is 714 kPa. This represents a considerable rigid soil. Therefore, it is supposed that the soil will not collapse. However, it has been checked that the capacity of the soil is not overpassed by any of the footings. The lateral capacity has not been verified owing to the rigidity of the soil. The normal and shear stress components of each of the footings have been calculated. It has been then obtained that none of the footings presents higher values of stresses than q_a in the vertical direction and at their bottom surfaces.

Additionally, the Von Misses (yielding) stress (σ_y) has been calculated to check if the footings will present plastic mechanisms. The normal and shear stress components of each of the footings have been obtained. For the X direction, σ_y has been 1 712 kPa. As shown in Fig. 21, two of the inner footings will yield, reaching this limit stress by 4%. In the Y direction, none of the footings present plastic behaviour. It can be seen that the number of footings that will present plastic mechanisms is not considerable and that this plasticity is only produced in certain locations at the border of the footings. Hence, it can be seen that the failure

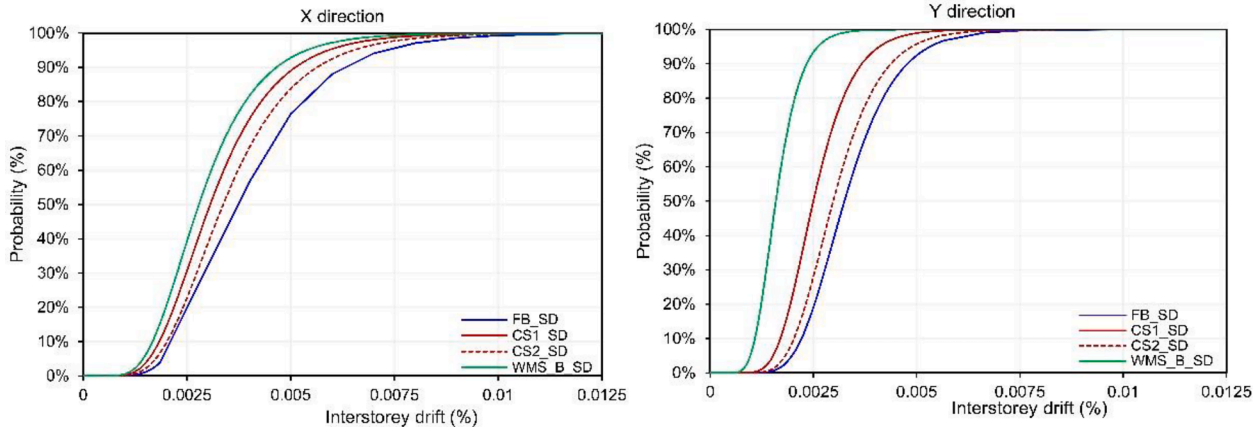

Fig. 20. Fragility curves for the SD LS considering the most representative results from the static analyses.

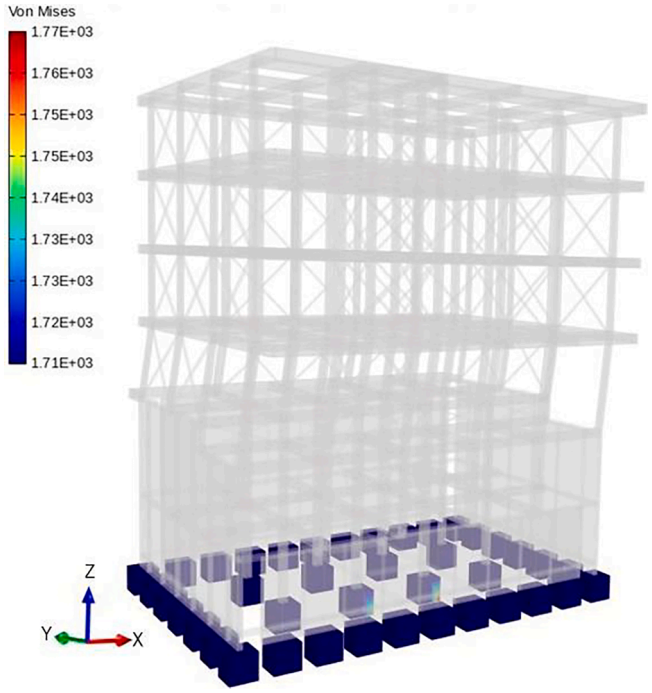

Fig. 21. Von Misses stress distribution for the model CS1 for the X direction for the ultimate displacement step.

is expected to happen due to the premature brittle failure of the RC frames rather than the activation of a plastic mechanism in the footings or the collapse of the surrounding soil.

6. Conclusions

This paper has focused on the assessment of the SSI effects in the seismic vulnerability analyses of RC buildings. A methodology to include and to quantify the SSI effects and their application to a real case study building in Lisbon have been presented. Owing to the lack of guidance available, this paper has been conceived as an opportunity to easily-include the SSI in the seismic analyses.

6.1. Specific conclusions

Specifically, in the light of the results obtained, the following has been concluded:

- Soil characterisation. A methodology to define the parameters needed to numerically model the soil considering two configurations has been posed. Moreover, the methodology presents two approaches based on laboratory and in situ tests, respectively. A clayey soil type has been defined considering two geotechnical investigations. The soil characterised can be commonly found in Lisbon.
- Superstructure modelling. The building selected is a mid-rise structure, representative of an important part of the Lisbon buildings' stock. In this study, it has been proved that it is affected by the *p-Δ* effects. These characteristics make this building prone to be affected by the SSI as defined by the EC8.
- BNWM analyses. The results show that modelling the footings is one of the most important aspects to obtain reliable results. These affect the initial stiffness and the maximum strength of the capacity curves. It has been concluded that the BNWM does not capture the real modal behaviour of the models. This is due to its inability to consider the masses of the footing and the soil, which can be important in future dynamic analyses. The softer response of the WMN model is mainly due to the fact that the foundation is not specifically modelled and the omission of the q-z springs owing to the software limitation. The foundation is only taken into account by the different stiffness coefficients used to define the nonlinear materials. Contrariwise, the WMS and WMB configurations, which modelled the foundations to certain extent, have been able to obtain better results. The WMS has obtained more similar values to the solid configurations. This configuration requires less modelling and computation time. It has been concluded that the ultimate capacities of the soil (p_{ult}, t_{ult} and q_{ult}) are the most important parameters affecting the behaviour of the buildings. Higher values of p_{ult} and t_{ult} lead to smaller displacements and higher shear forces in the capacity curves, respectively. These results have been obtained for a simple foundation configuration: shallow footings on a clayey soil and for a type of RC buildings. However, it should be pointed out that this could be worsen by bearing in mind the energy dissipation, as proved for more complex systems composed of groups of piles. The main parameters affecting these capacities are the Mohr-Coulomb strength parameters (ϕ, c) and, to a lesser extent, the soil weight, γ, the depth of the footings, D_f and their area. The stiffness of the footings is important in the case of *p-y* springs. *p-y* and *t-z* springs have been the most significant since they tend to capture the soil horizontal passive pressure and the slippage of the foundation on the soil, which is important in horizontal analyses.
- 3D direct modelling of soil. It has been concluded that coarse meshes and linear models of soil lead to rigid soil behaviours. Therefore, the models are not able to capture the soil flexibility, resulting in unreliable results. The reduction of the seismic capacity has not been as

high as in the BNWM configurations due to the lack of properties considered in those analyses: the presence of rigid and deep soil layers, the modelling of footings as solid, the consideration of the complete behaviour of the soil and the application of interactions to soil-footings surfaces. This is also due to the high values of V_s determined, which results in a very rigid soil. More soil parameters are needed to define the soil constitutive law in contrast to the method of springs. The differences in the periods (3%) of the models with solid soil is related to the different values of the soil weight (2%).

6.2. General conclusions

In general and based on the results of the RC building case study, it has been concluded that increasing the soil flexibility leads to higher periods and higher seismic damage. Therefore, by omitting the SSI effects, the initial and the strength capacity of the structures might be overestimated. For this case study, the maximum strength of the models can be reduced by up to 15% if the SSI effects are considered. According to the variability of the soil parameters, for the BNWM approach, there is a 10% variation of the maximum strength. Regarding the modal analyses, the dynamic characteristics of the models with the BNWM and the solid soil cannot be compared due to the inability to consider the masses of the footings and the soil in the first method.

The BNWM has been able to predict the behaviour of the structure similarly to the direct modelling of the soil if the footings are modelled. However, it might not be able to reproduce it if the soil were softer or if the analyses were performed under drained conditions (sand). This method does not take into account important aspects in drained analyses such as the dilatancy or the water presence. Moreover, in this case, the soil characterised has been very rigid. The affection of the SSI effects has, therefore, not been outstanding. However, the SSI affection can be higher for softer soils as proved in this research. Softer types of soil can be found in several parts of Lisbon. Hence, further research should be carried out in order to determine the SSI effects considering other types of soils and to other RC building structures and to prove the suitability of the models.

It is worth pointing out that if different values of dispersion had been adopted for the SSI fragility curves, the seismic performance of the buildings could have become much worse. It can be stated that, in the fragility analyses, the parameters affecting the BNWM are the Mohr-Coulomb strength parameters (ϕ, c) and, to a lower extent, the soil weight, γ, the depth of the footings, D_f and the area of the footings. In the case of the solid models, these are G and B, which are related to V_s and γ. As can be observed in these results and concluded from the state of the art, the characteristics of the footings affect the buildings' performance. In this research, they have not been varied. In order to define the statistical parameters for these models, different configurations varying these parameters should be also carried out.

The results show that the modal behaviour and the deformed shape of the building are the same with and without considering the SSI. Nevertheless, if the SSI effects are borne in mind, the damage in the structural elements occurs at lower displacements. Therefore, by considering the SSI, the damage is amplified. Hence, they might affect the retrofitting strategies of the buildings in terms of the amount of retrofitting material needed and the type of solution defined. In this case, none of the models complies with the EC8 restrictions. The columns located at the soft storey have been the first damaged. Moreover, the damage has be increased by up to 15% and 194% for the solid models and the BNWM configurations, respectively.

In this case, due to the main characteristics of these RC buildings, the failure is controlled by the behaviour of the superstructure. In particular, owing to the very low transversal reinforcement, this structure is subjected to the premature brittle shear failure of the vertical structural elements. The assessment of the failure has been carried out following the Eurocode 8 procedure. Additionally, the local failure of the footings has been checked. For this case, it has been obtained that only two inner footings will present plastic behaviour at their corners. Also, it has been checked that the allowable bearing capacity of the soil is not overpassed. However, for certain cases, the footings can become the critical aspect and it is recommended to include their local assessment in future analyses.

7. Future research work

For the assessment of the effects of the SSI, this study has focused on two SSI modelling approaches. However, other methods are available in the literature, whose effects and implementing could be also compared. To do so, correlation studies with experimental tests are needed to validate and calibrate new materials to be implemented in the software. In this work, the goal was to model some SSI approaches in OpenSees that are available in the literature, to study their effects, limitations and to obtain some conclusions on their implementation. Nonlinear static analyses have been carried out, which lead to certain limitations and assumptions compared to nonlinear dynamic analyses. However, they can provide realistic results for the case study building, a regular mid-rise building.

This work presents also certain limitations regarding the modelling of the SSI. Further research should be carried out following the Winkler method considering different configurations. Such is the case of using different types of springs and performing parametric analysis. Regarding the direct method, different types of contact materials can be used to define the interaction between the soil and the foundation.

Although the present results support the affection of the SSI in the seismic performance of the case study building, it should be mentioned that this work has been limited to one type of soil. Analyses considering other types of soil such as sandy and performing the analyses under drained conditions are needed to prove this statement. Additionally, more complex foundation systems should be also considered. In these configurations, other aspects such as the energy dissipation effects are more important rather than the lateral capacity.

The nonlinear behaviour of the RC frames has been simulated through the distributed plasticity approach. It could be useful to assess the performance by following the lumped method. Also, special attention should be carried out on the eventual shear-critical behaviour of the columns, which is the typical failure of RC elements. In this work, it has been simply analysed by following the seismic code requirements.

Additionally, owing to the unsafety of the case study building, retrofitting strategies could be added to improve its capacity considering the decrease of the capacity due to the SSI affection. These analyses could be expressed in terms of losses instead of just the structural assessment.

CRediT authorship contribution statement

M.V. Requena-Garcia-Cruz: Conceptualization, Methodology, Investigation, Formal analysis, Software, Writing – original draft, Writing – review & editing. **R. Bento:** Conceptualization, Methodology, Supervision, Writing – review & editing, Funding acquisition. **P. Durand-Neyra:** Writing – review & editing, Supervision. **A. Morales-Esteban:** Writing – review & editing, Supervision, Funding acquisition.

Declaration of Competing Interest

The authors declare that they have no known competing financial interests or personal relationships that could have appeared to influence the work reported in this paper.

Acknowledgements

This work has been supported by the VI-PPI of the University of Seville by the granting of a scholarship. The grant provided by the Instituto Universitario de Arquitectura y Ciencias de la Construcción is acknowledged. The support of the Spanish Ministry of Science and Innovation through the PID2020-117207RB-I00 project is aknowledged. The second author would like to acknowledge the support of Fundação para a Ciência e a Tecnologia (FCT, Ministério da Educação e Ciência, Portugal) through the FCT Research Program: MitRisk - Framework for seismic risk reduction resorting to cost-effective retrofitting solutions, POCI-01-01456-Feder-031865.

References

[1] Kwag S, Ju BS, Jung W. Beneficial and detrimental effects of soil-structure interaction on probabilistic seismic hazard and risk of nuclear power plant. Adv Civ Eng 2018;2018:1–18.
[2] Jeong SY, Kang T-K, Yoon JK, Klemencic R. Seismic performance evaluation of a tall building: practical modeling of surrounding basement structures. J Build Eng 2020;31:101420. https://doi.org/10.1016/j.jobe.2020.101420.
[3] Anand V, Satish Kumar SR. Seismic soil-structure interaction: a state-of-the-art review. Structures 2018;16:317–26. https://doi.org/10.1016/j.istruc.2018.10.009.
[4] European Union. Eurocode 8: Design of structures for earthquake resistance. Part 1: General rules, seismic actions and rules for buildings. Belgium: 2004.
[5] Miranda E, Bertero VV. Evaluation of strength reduction factors for earthquake-resistant design. Earthq Spectra 1994;10(2):357–79. https://doi.org/10.1193/1.1585778.
[6] Karapetrou ST, Fotopoulou SD, Pitilakis KD. Seismic vulnerability assessment of high-rise non-ductile RC buildings considering soil-structure interaction effects. Soil Dyn Earthq Eng 2015;73:42–57. https://doi.org/10.1016/j.soildyn.2015.02.016.
[7] Diário do Governo. Regulamento de Segurança e Acções para Estruturas de Edifícios e Pontes (RSA), Decreto-Lein. 235/83, Lisbon, Portugal [In Portuguese]. 1983.
[8] Instituto Nacional de Estatística (INE). "Censos 2011 Resultados Definitivos - Portugal" , I.P. Lisboa [In Portuguese]. 2012. http://censos.ine.pt/.
[9] Couto R, Requena-García-Cruz MV, Bento R, Morales-Esteban A. Seismic capacity and vulnerability assessment considering ageing effects: case study—three local Portuguese RC buildings. Bull Earthquake Eng 2021;19(15):6591–614.
[10] Silva V, Crowley H, Varum H, Pinho R. Seismic risk assessment for mainland Portugal. Bull Earthq Eng 2015;13(2):429–57. https://doi.org/10.1007/s10518-014-9630-0.
[11] Caruso C, Bento R, Castro JM. A contribution to the seismic performance and loss assessment of old RC wall-frame buildings. Eng Struct 2019;197:109369. https://doi.org/10.1016/j.engstruct.2019.109369.
[12] Saitoh M. Simple model of frequency-dependent impedance functions in soil-structure interaction using frequency-independent elements. J Eng Mech 2007;133(10):1101–14. https://doi.org/10.1061/(ASCE)0733-9399(2007)133:10(1101).
[13] Pisanò F, Flessati L, Di Prisco C. A macroelement framework for shallow foundations including changes in configuration. Géotechnique 2016;66(11):910–26.
[14] Li Z, Kotronis P, Escoffier S, Tamagnini C. A hypoplastic macroelement for single vertical piles in sand subject to three-dimensional loading conditions. Acta Geotech 2016;11(2):373–90.
[15] Salciarini D, Tamagnini C. A hypoplastic macroelement model for shallow foundations under monotonic and cyclic loads. Acta Geotech 2009;4(3):163–76. https://doi.org/10.1007/s11440-009-0087-2.
[16] Ramirez J, Barrero AR, Chen L, Dashti S, Ghofrani A, Taiebat M, et al. Site response in a layered liquefiable deposit: evaluation of different numerical tools and methodologies with centrifuge experimental results. J Geotech Geoenvironmental Eng 2018;144(10):04018073. https://doi.org/10.1061/(ASCE)GT.1943-5606.0001947.
[17] Hyeon Chai S, Kwon O-S. Implementation of the intensity and frequency dependent shallow foundation element in OpenSees. 12th Can. Conf. Earthq. Eng., Quebec: 2019, p. 1–8.
[18] Harden CW, Hutchinson TC. Beam-on-nonlinear-winkler-foundation modeling of shallow, rocking-dominated footings. Earthq Spectra 2009;25(2):277–300. https://doi.org/10.1193/1.3110482.
[19] Boulanger RW, Curras CJ, Kutter BL, Wilson DW, Abghari A. Seismic soil-pile-structure interaction experiments and analyses. J Geotech Geoenvironmental Eng 1999;125(9):750–9.
[20] Rahmani A, Taiebat M, Finn WDL, Ventura CE. Evaluation of p-y springs for nonlinear static and seismic soil-pile interaction analysis under lateral loading. Soil Dyn Earthq Eng 2018;115:438–47. https://doi.org/10.1016/j.soildyn.2018.07.049.
[21] Sharma N, Dasgupta K, Dey A. Optimum lateral extent of soil domain for dynamic SSI analysis of RC framed buildings on pile foundations. Front Struct Civ Eng 2020;14(1):62–81. https://doi.org/10.1007/s11709-019-0570-2.
[22] Raychowdhury P, Hutchinson TC. Performance evaluation of a nonlinear Winkler-based shallow foundation model using centrifuge test results. Earthq Eng Struct Dyn 2009;38:679–98. https://doi.org/10.1002/eqe.902.
[23] Rajeev P, Tesfamariam S. Seismic fragilities of non-ductile reinforced concrete frames with consideration of soil structure interaction. Soil Dyn Earthq Eng 2012;40:78–86. https://doi.org/10.1016/j.soildyn.2012.04.008.
[24] Raychowdhury P, Jindal S. Shallow foundation response variability due to soil and model parameter uncertainty. Front Struct Civ Eng 2014;8(3):237–51. https://doi.org/10.1007/s11709-014-0242-1.
[25] Behnamfar F, Banizadeh M. Effects of soil-structure interaction on distribution of seismic vulnerability in RC structures. Soil Dyn Earthq Eng 2016;80:73–86. https://doi.org/10.1016/j.soildyn.2015.10.007.
[26] Khatibinia M, Salajegheh E, Salajegheh J, Fadaee MJ. Reliability-based design optimization of reinforced concrete structures including soil–structure interaction using a discrete gravitational search algorithm and a proposed metamodel. Eng Optim 2013;45(10):1147–65. https://doi.org/10.1080/0305215X.2012.725051.
[27] Maslenikov 0. R., Chen AJC, Johnson JJ. Uncertainty in Soil-Structure Interaction-Analysis Arising from Differences in Analytical Techniques. CA (USA): Lawrence Livermore National Lab; 1982.
[28] Cayci BT, Inel M, Ozer E. Effect of soil-structure interaction on seismic behavior of mid-and low-rise buildings. Int J Geomech 2021;21(3):04021009. https://doi.org/10.1061/(ASCE)GM.1943-5622.0001944.
[29] Abd-Elhamed A, Mahmoud S. Simulation analysis of TMD controlled building subjected to far- and near-fault records considering soil-structure interaction. J Build Eng 2019;26:100930. https://doi.org/10.1016/j.jobe.2019.100930.
[30] Sáez E, Lopez-Caballero F, Modaressi-Farahmand-Razavi A. Effect of the inelastic dynamic soil–structure interaction on the seismic vulnerability assessment. Struct Saf 2011;33(1):51–63.
[31] Pitilakis KD, Karapetrou ST, Fotopoulou SD. Consideration of aging and SSI effects on seismic vulnerability assessment of RC buildings. Bull Earthq Eng 2014;12(4):1755–76.
[32] Requena-Garcia-Cruz MV, Couto R, Bento R, Morales-Esteban A. Influence of vertical irregularities on the seismic assessment of RC framed and wall-frame buildings. 9th Eur. worshop Seism. Behav. Irregul. complex Struct., Lisbon, Portugal: 2020.
[33] Ruiz SE, Santos-Santiago MA, Bojórquez E, Orellana MA, Valenzuela-Beltrán F, Bojórquez J, et al. BRB retrofit of mid-rise soft-first-story RC moment-frame buildings with masonry infill in upper stories. J Build Eng 2021;38:101783. https://doi.org/10.1016/j.jobe.2020.101783.
[34] Requena-Garcia-Cruz M-V, Morales-Esteban A, Durand-Neyra P, Zapico-Blanco B. Influence of the constructive features of RC existing buildings in their ductility and seismic performance. Bull Earthq Eng 2021;19(1):377–401. https://doi.org/10.1007/s10518-020-00984-z.
[35] Villar-Salinas S, Guzmán A, Carrillo J. Performance evaluation of structures with reinforced concrete columns retrofitted with steel jacketing. J Build Eng 2021;33:101510. https://doi.org/10.1016/j.jobe.2020.101510.
[36] Laranjo M. Argilas miocénicas de Lisboa. Parametrização para o dimensionamento de estruturas geotécnicas. Universidade do Porto, 2013.
[37] Pinto da Silva AM. Caracterização Geológica e Geotécnica da área compreendida entre o Lumiar e o Olival Basto. Uniersidade de Lisboa 2015.
[38] Laboratório Nacional de Energia e Geologia (LNEG). Carta Geologica do Concelho de Lisboa. Lisbon, Portugal: 2020.
[39] AENOR. UNE-EN ISO 1468: Geotechnical investigation and testing - Identification and classification of soil - Part 1: Identification and description (Asociacion Española de Normalizacion y Certificacion). 2019.
[40] Bang E-S, Kim D-S. Evaluation of shear wave velocity profile using SPT based uphole method. Soil Dyn Earthq Eng 2007;27(8):741–58.
[41] Naik SP, Patra NR, Malik JN. Spatial distribution of shear wave velocity for late quaternary alluvial soil of Kanpur city, Northern India. Geotech Geol Eng 2014;32(1):131–49. https://doi.org/10.1007/s10706-013-9698-3.
[42] McKenna F, Fenves GL, Scott MH. OpenSees: Open system for earthquake engineering simulation. Pacific Earthquake Engineering Research Center 2000.
[43] Petracca M, Candeloro F, Camata G. STKO user manual. Pescara, Italy: ASDEA Software Technology; 2017.
[44] Calabrese A, Almeida JP, Pinho R. Numerical issues in distributed inelasticity modeling of RC frame elements for seismic analysis. J Earthquake Eng 2010;14(sup1):38–68.
[45] Mander JB, Priestley MJN, Park R. Theoretical stress-strain model for confined concrete. J Struct Eng 1988;114(8):1804–26. https://doi.org/10.1061/(ASCE)0733-9445(1988)114:8(1804).
[46] Caruso C, Bento R, Sousa R, Correia AA. Modelling strain penetration effects in RC walls with smooth steel bars. Mag Concr Res 2019;71(17):894–906. https://doi.org/10.1680/jmacr.18.00052.
[47] Celarec D, Ricci P, Dolšek M. The sensitivity of seismic response parameters to the uncertain modelling variables of masonry-infilled reinforced concrete frames. Eng Struct 2012;35:165–77. https://doi.org/10.1016/j.engstruct.2011.11.007.
[48] Dolšek M, Fajfar P. The effect of masonry infills on the seismic response of a four storey reinforced concrete frame-a probabilistic assessment. Eng Struct 2008;30(11):3186–92. https://doi.org/10.1016/j.engstruct.2008.04.031.
[49] Thomas JM, Gajan S, Kutter BL. Soil-Foundation-Structure Interaction: Shallow Foundations. Centrifuge Data Report for the SSG04 Test Series. 2005.
[50] Raychowdhury P. Nonlinear Winkler-based Shallow Foundation Model for Performance Assessment of Seismically Loaded Structures. University of California; 2008.
[51] Gazetas G. Chapter 15: Foundation Vibrations. In: Fang HY, Reinhold VN, editors. Found. Eng. Handb. 2nd ed., New York: 1991, p. 553–93.
[52] Bentley Systems. PLAXIS Manual 2021.
[53] Mazzoni S, McKenna F, Scott MH, Fenves GL. OpenSees command language manual. 2006.

[54] Yang Z, Elgamal A. Command Manual and User Reference for OpenSees Soil Models and Fully Coupled Element. San Diego: 2003.
[55] European Union. Eurocode-8: Design of structures for earthquake resistance. Part 3: Assessment and retrofitting of buildings. Brussels, Belgium: 2005.
[56] IPQ. Eurocódigo 8: Projeto de estruturas para resisteência aos sismos. Parte 3: Avaliaçao e reabilitaçao de edificios, NP EN 1998-3:2017 (Instituto Português da Qualidade) (IPQ in Portuguese). 2017.
[57] Silva V, Crowley H, Varum H, Pinho R, Sousa L. Investigation of the characteristics of Portuguese regular moment-frame RC buildings and development of a vulnerability model. Bull Earthq Eng 2015;13(5):1455–90. https://doi.org/10.1007/s10518-014-9669-y.
[58] Sakellariadis L, Anastasopoulos I, Gazetas G. Fukae bridge collapse (Kobe 1995) revisited: new insights. Soils Found 2020;60(6):1450–67.
[59] Tomeo R, Bilotta A, Pitilakis D, Nigro E. Soil-structure interaction effects on the seismic performances of reinforced concrete moment resisting frames. Procedia Eng 2017;199:230–5.